PORE-SIZE DISTRIBUTION OF STANNIC OXIDE IN POWDER, CERAMIC AND GEL FORMS

By

THEODOROS GALACTION VERNARDAKIS

Bachelor of Science

College of Emporia

Emporia, Kansas

1965

Submitted to the Faculty of the Graduate College
of the Oklahoma State University
in partial fulfillment of the requirements
for the Degree of
MASTER OF SCIENCE
May, 1968

PORE-SIZE DISTRIBUTION OF

STANNIC OXIDE IN POWDER,

CERAMIC AND GEL FORMS

Thesis Approved:

Clarence M. Cunningham
Thesis Adviser

O C Dermer

D Durham
Dean of the Graduate College

ACKNOWLEDGMENT

The author wishes to express his gratitude to Drs. C. M. Cunningham and E. E. Kohnke for initially suggesting the area of study and for their valuable guidance during the investigation; to the National Aeronautics and Space Administration for sponsoring the research (NASA Grant NsG - 609) in the form of a research assistantship; to Oklahoma State University for aid in the form of a teaching assistantship, and to the Oklahoma State University Research Foundation for their administrative assistance.

TABLE OF CONTENTS

LIST OF TABLES

LIST OF FIGURES

CHAPTER I

INTRODUCTION

The physical structure of finely divided and porous materials is of great importance in studies of catalysis. Investigations dealing with the size of the pores in such materials have been carried out extensively in recent years. Brunauer, Emmett, and Teller[1] (BET) and also Harkins and Jura[2] have laid the foundations for such studies with their theories of physical adsorption, which have been proven very successful in determining the specific surface areas of adsorbents from gas adsorption data.

These theories, excellent as they are in obtaining surface areas, are inadequate in the treatment of some frequently occurring isotherm phenomena. They have been supplemented, in this respect, by the introduction of the theory of "capillary condensation" which takes place in the fine pores of solid adsorbents, mainly due to Cohan[3] and Brunauer[4]. The modern theory of adsorption, due to Wheeler[5,6], combines both the BET multimolecular adsorption and the capillary condensation viewpoints.

The study of capillary condensation phenomena, which occur at low relative pressures, is the primary source of information about the size of the pores in solid adsorbents. Multilayer adsorption takes place simultaneously with condensation in the capillaries. In the calculations of pore-size distributions this type of adsorption is to be left out as not arising from the filling of the pores so that corrections for

it are necessary.

If a definite pore geometry is assumed and if the Kelvin equation is considered applicable to capillaries of a nature such as that of porous solids then distributions of pore size can be easily evaluated. Several methods have been developed to deal with this type of computation. The most important of them will be reviewed in Chapter III.

It is the purpose of the present investigation to study the nature of the pores in finely divided and porous substances and also to obtain pore-size distributions from considerations of capillary condensation. The material selected for this study is stannic oxide in the forms of powder, ceramic, and gel. Nitrogen adsorption isotherms together with their specific surface areas obtained from the BET method, at 78°K (liquid nitrogen), are used to furnish the data necessary for the calculations.

The powder, ceramic, and gel are expected to differ considerably in their pore-size distributions. These differences will be brought out and discussed in terms of the special shape of the adsorption isotherm for each, and conclusions will be drawn as to the correlation between the type of the isotherm and the manner by which the filling of the pores is taking place. The cumulative surface areas which are obtained by this method are compared with the values from the BET method.

CHAPTER II

THEORY OF ADSORPTION IN PORES AND CAPILLARIES

Modern theories[5,6] regard physical adsorption as arising from contributions of both multilayer adsorption and capillary condensation in contrast to the older theories which attributed adsorption either entirely to capillary condensation or entirely to multilayer adsorption[4].

Adsorbed films in multilayer adsorption are considered to arise from the interactions between the surface of the adsorbent and the molecules of the adsorbate due to van der Waals forces. Multilayer films are formed on the "flat" surface of the adsorbent and they increase in number as the relative pressure approaches unity, while on the inner walls of the capillaries the thickness of these layers would increase until such capillaries are filled[7].

Capillary condensation, on the other hand, is due to the action of surface tension at a curved meniscus. This surface tension lowers the equilibrium vapor pressure p, at the meniscus, below that of the bulk liquid p_o, according to the Kelvin equation[7].

Pierce and Smith[8] have recognized two types of capillaries depending on the value of the relative pressure at which they fill. The first type includes capillaries which fill at a low relative pressure (below 0.5) while the second type includes those which fill at a relative pressure between 0.5 and 1.0. These two types exhibit different adsorption isotherms. On desorption the former show no hysteresis,

while the latter do. Figure 1 shows the general nature of the isotherms for the two types of capillaries together with the S-shaped isotherm for "nonporous" solids. The isotherm for the first class of capillaries is represented by curve A, and that for the second class by curve B, while curve C gives the isotherm for nonporous solids. These isotherms have been designated by Brunauer as type I (Langmuir type) without hysteresis for A and type II with and without hysteresis for B and C respectively.

Two ways have been recognized to be responsible for the filling of capillaries. The first takes place through condensation of the vapor at the meniscus which bridges the walls of the pore. The second takes place through the building up of a multilayer film until all the space of the capillary is filled. A third way is the one that combines both. A pore can start filling with a layer on its inner wall and after the layers on opposite walls meet and merge it will end up with a meniscus. Determination as to the effectiveness of these processes during adsorption comes from considerations of both size and shape of the capillaries.

For very narrow pores, of which each one can be bridged either by a single molecule or by a monomolecular film on each wall, condensation starts at the very beginning of adsorption. This type of pores are filled at a very low relative pressure and substances which have pores such as these exhibit a Brunauer type I adsorption isotherm without hysteresis (Figure 1, curve A). The reason for the absence of hysteresis comes from the fact that adsorption and desorption occur in the same manner, from a meniscus. For these highly porous solids, after all pores have been filled, the isotherm rises but insignificantly which indicates that contributions from any "flat" surface in the solid are of minor importance.

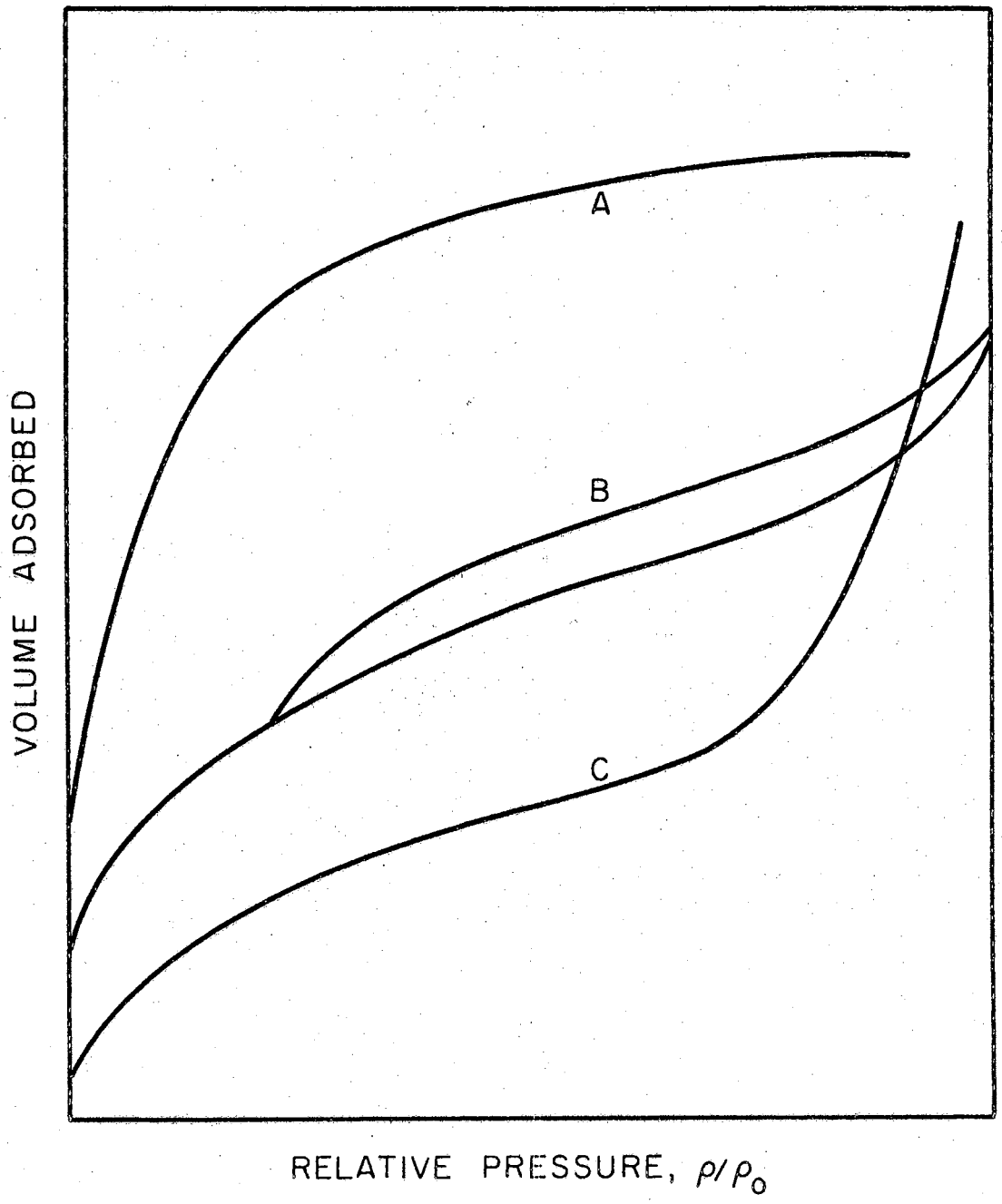

Figure 1. Typical Adsorption Isotherms: A, Brunauer's Type I or Langmuir Type; B, Type II with Hysteresis; C, Type II Without Hysteresis or S-shaped.

For pores which are relatively wide a monomolecular film on each wall will not be able to bridge one such pore. In this case adsorption takes place as a monomolecular layer on the inner walls of the pore, an effect which is the same as that for a flat surface. The isotherms of materials having this type of pores are exactly like those of nonporous solids at very low relative pressure. When a value of this pressure is reached at which the wall films start merging together, condensation begins in the capillaries and the surface diminishes owing to the filling of pores. This process continues to take place as the relative pressure increases toward unity. As the molecular layers in a single pore meet and merge together, the forces acting on the molecules of the new combined layer become stronger. The explanation of this effect comes from the fact that these molecules are now held on and between two walls instead of only one as in the case before merging occurred. They are therefore more strongly bound than previously because forces twice as strong are acting upon them. Consequently, removal of these molecules from the meniscus during desorption takes place at a lower relative pressure than the original adsorption which was building up in the form of a single wall film. A result of the above is the hysteresis which is observed during desorption as shown by curve B of Figure 1. This represents a type II isotherm with hysteresis.

The absence of pores, as in "nonporous" solids, gives rise to an S-shaped adsorption isotherm. This corresponds to Brunauer's type II isotherm without hysteresis (Figure 1, curve C). The term "nonporous" is not entirely correct because in such solids some capillaries may be present along with a large "flat" or "free" surface. In this case the presence of capillaries causes condensation at very low relative

pressure and at the beginning of adsorption the isotherm is not very mcuh different, although flatter, than the type I isotherm for highly porous materials. For such solids as the size of the pores increases the isotherm becomes steeper at higher values of the relative pressure. When adsorption on the "flat" surface takes over the isotherm starts getting steeper and becomes very steep at high pressure. On desorption no hysteresis is observed because molecules are removed from the "flat" surface in the same manner and at the same pressure of the original adsorption.

An S-shaped isotherm therefore is not a conclusive indication that a solid is completely nonporous. Capillaries will be present and they can be detected if such an isotherm is compared with isotherms for true nonporous solids. The effect of these capillaries is to lower the isotherm below the nonporous isotherm. Calculations of pore size distributions for materials of this nature and with an S-shaped isotherm will show that capillaries are present in varying numbers.

Fine powders and ceramics, in general, exhibit this type of isotherm. When the adsorption isotherm of a powder is compared with the adsorption isotherm of the corresponding ceramic it is usually found that the isotherm of the latter lies below that of the former because of the lower porosity of the ceramic. Such an effect is expected from the special considerations of the preparation of ceramics. During the sintering process, which consists of pressing and firing of the powder, pores in the resulting ceramic become smaller and fewer with simultaneous decrease in the "free" surface available for adsorption.

CHAPTER III

METHODS OF PORE-SIZE DISTRIBUTION CALCULATIONS

Several methods dealing with the mathematical evaluation of the size of pores in finely divided and porous materials have been advanced in recent years. These methods, as mentioned previously, are based on the theories of physical adsorption, the most important of which is that of Brunauer, Emmett, and Teller[1]. The theory of Wheeler[5,6], which combines both multilayer adsorption and capillary condensation, gives a better picture of physical adsorption. Application of this theory to the experimental isotherms, with the necessary corrections for multimolecular adsorption, constitutes the basis upon which pore-size distributions are evaluated. The experimental isotherms are usually taken to be the ones determined by the BET method from nitrogen gas adsorption data.

The starting point for all calculations of this type is the Kelvin equation for a cylindrical capillary model in the following form:

$$\ln(P/P_o) = -(2\sigma V_m \cos \Psi / RTr_k) \qquad (3\text{-}1)$$

where (P/P_o) is the relative presure, σ is the surface tension of the liquid adsorbate, V_m is the molar volume of the liquid adsorbate, Ψ is the contact angle between the surface of the adsorbed liquid and the wall of the capillary (usually taken as zero), R is the ideal gas constant, T is the temperature of the liquid, and r_k is the Kelvin radius.

Methods of calculation corresponding to either cylindrical or slit-shaped pores have been developed by a number of investigators. A review of the most important of these methods will be presented, first for a cylindrical and then for a parallel plate model.

Barrett, Joyner, and Halenda[9] using the model proposed by Wheeler developed a method for circular pores which is rather complicated and time-consuming. Their theory is given by the equation

$$V_s - V = \pi \int_{r_{p_n}}^{\infty} (r-t)^2 L(r) dr \qquad (3\text{-}2)$$

where V_s is the volume of nitrogen gas adsorbed at the saturation pressure P_o, V is the volume of gas adsorbed at the equilibrium pressure P, $L(r)dr$ is the total length of pores with radii between r and r + dr, r_{p_n} is the radius of the largest pore filled with liquid nitrogen at any pressure (critical radius), and t is the thickness of the multilayer.

The above equation is simplified by taking stepwise decrements of the relative pressure (P/P_o) on the desorption isotherm starting at $P/P_o = 1$. The equation becomes

$$V_{p_n} = R_n V_n - R_n t_n \sum_{j=1}^{n-1} c_j A_{p_j} \qquad (3\text{-}3)$$

where V_{p_n} is the pore volume at any particular pressure, V_n is the observed volume of gas desorbed, t_n is the amount of reduction in the thickness of the adsorbed layer, A_{p_j} is the area of each pore at any particular pressure p_j, and n is the number of relative pressure incre-

ments. R_n and c_j are given by the equations

$$R_n = r_{p_n}^2 / (r_{k_n} + t_n)^2$$

and

$$c_j = (\bar{r}_p - \bar{t}_r)/\bar{r}_p$$

where r_{p_n} is the pore radius at pressure p_n, r_{k_n} is the Kelvin radius, and $\bar{t}_r$ is the thickness of the adsorbed layer at the corresponding value of P/P_o.

The above equation for V_{p_n} depends only on the two following assumptions: (1) the pores are cylindrical and (2) the amount of adsorbate in equilibrium with the gas phase is retained by the adsorbent either by physical adsorption on the pore walls or by capillary condensation in the inner capillary volume. This method is generally more applicable but there are a lot of approximations necessary and it is also rather time-consuming.

C. G. Shull[10] has applied the Wheeler theory to experimental isotherm data which he compares with standard isotherms represented either by Maxwellian or by Gaussian distribution functions. The reason for this is that the layer thicknesses of the BET theory become much larger than the experimental thicknesses for flat surfaces in the region of high pressure.

Shull in his method uses the simplified equation of the Wheeler theory, i.e.,

$$V_s - V = \pi \int_{r_p}^{\infty} (r-t)^2 L(r) dr \qquad (3\text{-}2)$$

where r_p is the corrected Kelvin radius obtained as a function of the relative pressure from the Kelvin equation and from the equation

$$r_p = t + r_k \tag{3-4}$$

which gives the radius of a cylindrical capillary at a particular value of the pressure. The quantity $(V_s - V)$ gives the volume of gas which is not yet adsorbed at a pressure p. This volume is simply equal to the total volume of pores which have not as yet been filled at that same pressure p.

The pore-size distribution function L(r) can be represented by a Maxwellian distrubution function, given by:

$$L(r) = Ar \cdot \exp(-r/r_o) \tag{3-5}$$

with A and r_o being constants. When L(r) is substituted into the Wheeler equation and the integration is performed the expression for (V_s-V) is obtained in the form:

$$V_s - V = Ar_o^4 \cdot M(r_p, r_o) \tag{3-6}$$

where

$$M(r_p, r_o) = (\pi/r_o^3)\exp(-r_p/r_o) \left[r_p(r_p-t)^2 + 6r_o^3 + 2r_o^2(3r_p-2t) + r_o(3r_p-t)(r_p-t) \right] \tag{3-7}$$

The above function is evaluated at various values of r_p and r_o and a family of curves, known as "standard inverted isotherms", is obtained when plotting $M(r_p, r_o)$ versue r_p.

The function L(r) may also be represented by a Gaussian distribu-

tion function as:

$$L(r) = Ae^{-\left[\beta/r_o(r-r_o)\right]^2} \tag{3-8}$$

with A, β, and r_o being constants. Substitution of L(r) into the Wheeler expression for (V_s-V) and integration gives:

$$V_s - V = 2A(r_o^3/\beta)G\beta(r_p,r_o) \tag{3-9}$$

where

$$G\beta(r_p,r_o) = \frac{\pi}{4r_o^2}\{\frac{r_o}{\beta}(r_p - 2t + r_o)e^{-\rho^2} + \tag{3-10}$$

$$\sqrt{\pi}\left[1 - H(\rho)\right]\left[(r_o - t)\right]^2 + \tfrac{1}{2}(r_o/\beta)^2\}$$

and ρ and H(x) are given by:

$$\rho = (\beta/r_o)(r_p-r_o) \quad \text{and} \quad H(x) = (2/\sqrt{\pi})\int_0^x e^{-y^2}dy$$

The parameter β determines the width of the pore-size distribution while r_o determines the average pore size. The function $G\beta(r_p,r_o)$ is is evaluated for various values of the parameters β, r_p, and r_o and a family of Gaussian "standard inverted isotherms" is obtained when $G\beta(r_p,r_o)$ is plotted versus r_p. In this case β has a constant value while r_p and r_o change; in other words $G\beta(r_p,r_o)$ is evaluated at certain values of β with r_p and r_o changing for every different value of β.

In order to interpret the experimental data the following procedure is used: The experimental isotherm is plotted as V_s-V (using a logarithmic scale) versue r_p, the corrected Kelvin radius. This is referred to as an "inverted isotherm", which in turn is matched with either a Maxwellian or a Gaussian "standard inverted isotherm." The pore-size

distribution L(r) would be known immediately if an acceptable match is obtained between the "inverted" and the "standard inverted" isotherms because the parameters of the standard isotherm are known.

Oulton[11] suggested a method for calculating the pore-size distribution from a desorption isotherm which considers the thickness of the adsorbed film that is attracted to the solid surface by forces greater than the interaction forces of the liquid itself. He assumes that the thickness of the film is constant and equal to the number of molecular layers at the relative pressure at which capillary condensation starts. He further assumes that the radius of the smallest pore present is determined at the closing of the hysteresis loop, i.e., at the pressure P/P_o where condensation sets in the capillaries. He defines the quantity Nd as being the thickness of the adsorbed film, where N is the number of molecular layers in the film and d is the diameter of a single molecule or the thickness of the monolayer. The value of Nd is the determining factor concerning the size of the pores and it is assumed that there are very few, if any, pores present with radii less than Nd. The calculation of the pore-size distribution therefore starts at the value of the lowest relative pressure at which hysteresis starts and pores whose radii are less than Nd are neglected completely.

Anderson[12], with the assumptions of Wheeler and Barrett, and Joyner and Halenda, has developed a method of numerical differentiation in obtaining differential pore distributions. The volume of pores emptied, V, is a function of the volume adsorbed, $V_{ads.}$, and the thickness of the monolayer, t, i.e.,

$$V = f(V_{ads.}, t) \qquad (3\text{-}11)$$

The differential volume of the pores emptied, dV, is then related to a differential amount desorbed, $dV_{ads.}$, by applying partial differentiation on the function of V. This method is developed fully in the original paper and it has been used very successfully to compute pore-size distribution curves on the assumption that pores are cylindrical in shape. Surface areas of adsorbents, such as silica gel, porous glass, alumina, etc., obtained by this method are in good agreement with the BET results with errors in the range of 3 to 10 per cent.

Methods of calculation of pore-size distributions for "silt-shaped" pores (parallel-plate model) were proposed by Innes[13] and De Boer[14] and co-workers in a series of articles[15,16,17].

Innes[13] regards the capillary system as being equivalent to a system of parallel plates with varying distances of wall separation. The Kelvin equation is still assumed to be applicable in this case, except that now the pore radius is replaced by the pore wall separation. It will be shown later that this separation is given by:

$$d = r_k + 2t \tag{3-12}$$

In his method Innes assumes that the total volume adsorbed, in cm^3 of liquid, denoted by X, is given by:

$$X = V + At \tag{3-13}$$

where V is the volume (in cm^3) of the pores that are completely filled with liquid nitrogen, and A is the surface area of the incompletely filled pores (in cm^2 per gram of adsorbent).

When very small increments are considered the equation for X can be written in the form

$$\Delta X = \Delta V + \bar{A}\Delta t + \bar{t}\Delta A \tag{3-14}$$

and

$$\Delta V = \frac{-\bar{d}\Delta A}{2} \tag{3-15}$$

where the bars denote average values over the particular increment under consideration.

Substitution of the equation for ΔV into that for ΔX gives

$$\Delta X = \Delta V + \bar{A}\Delta t - \frac{2\bar{t}}{d}(\Delta V) \tag{3-16}$$

or

$$\Delta V = \frac{\bar{d}}{\bar{d}-2\bar{t}}(\Delta X - \bar{A}\Delta t) \tag{3-17}$$

The assumption is then made that at the highest relative pressure, $(P/P_o) = 1$, all the pores are filled, so that $A = 0$ and $V = X$, and the pore size distribution can be evaluated by a stepwise procedure when equal increments of P/P_o are chosen on the desorption isotherm.

Lippens, Linsen, and De Boer[15,16,17] in their calculations of distribution curves for several aluminum oxide systems make use of the same wall separation term d , proposed by Innes, assuming that the pores in such oxides are "slit-shaped." The assumption that all the pores are filled at a relative pressure of unity is still valid, and starting at that pressure the desorption isotherm is divided into parts corresponding to equal steps of $2\Delta x$, with x used to denote P/P_o ($x = P/P_o$).

At the beginning of the $\underline{i}^{th}$ step the relative pressure is $x_i + \Delta x$, the volume adsorbed in cm^3 of liquid nitrogen is $X_{(x_i + \Delta x)}$, the surface area of that part of pores which are not filled with liquid nitrogen is

$S_{(x_i + \Delta x_i)}$, and the layer thickness is $t_{(x_i + \Delta x_i)}$. If the relative pressure is lowered to $x_i - \Delta x$ then the pores with Kelvin radius between $r_{k(x_i + \Delta x)}$ and $r_{k(x_i - \Delta x)}$ are emptied. The average Kelvin radius for this group of pores at x_i may be taken as $(r_k)_{x_i}$ if the single increment Δx is very small. The average wall separation or pore width at x_i is:

$$d_{x_i} = (r_k)_{x_i} + 2t_{x_i} \tag{3-18}$$

where t_{x_i} is the thickness of the adsorbed layer at x_i. The surface area of these pores is ΔS_{x_i} and their volume is given by:

$$\Delta V_{x_i} = \frac{1}{2} d_{x_i} \cdot \Delta S_{x_i} \tag{3-19}$$

At a relative pressure of $x_i - \Delta x$, which corresponds to the end of the $\underline{i}^{th}$ step, $X_{(x_i - \Delta x)}$ is the volume of nitrogen adsorbed, $S_{(x_i - \Delta x)}$ is the surface area of the pores not completely filled with liquid nitrogen, and $t_{(x_i - \Delta x)}$ is the layer thickness.

Therefore

$$\Delta X_{x_i} = X_{(x_i + \Delta x)} - X_{(x_i - \Delta x)} \tag{3-20}$$

where ΔX_{x_i} is the volume of nitrogen desorbed during the $\underline{i}^{th}$ step.

There are two contributions to the volume ΔX_{x_i}. The first is the volume due to capillary evaporation from the group of pores at x_i and from the decrease of the adsorbed layer thickness of the group of pores when the relative pressure is lowered x_i to $x_i - \Delta x$. This volume is

given by:

$$\frac{1}{2}\left[d_{x_i} - 2t_{(x_i - \Delta x)}\right] \cdot \Delta S_{x_i} \tag{3-21}$$

The second contribution is the volume that comes from the decrease of the adsorbed layer thickness in the pores which are emptied when the pressure $x_i + \Delta x$, is lowered to $x_i - \Delta x$, and it is equal to:

$$\left[t_{(x_i + \Delta x)} - t_{(x_i - \Delta x)}\right] \cdot S_{(x_i + \Delta x)} \tag{3-22}$$

where $S_{(x_i + \Delta x)}$ is obtained from the summation of all contributions ΔS_x of the groups of pores that have a width greater than $d_{(x_i + \Delta x)}$ or greater than $d_{(x_{i+1} - \Delta x)}$ since:

$$d_{(x_i + \Delta x)} = d_{(x_{i+1} - \Delta x)} \tag{3-23}$$

Therefore

$$S_{(x_i + \Delta x)} = \sum_i \Delta S_{(x_i - 1)} \tag{3-24}$$

and the equation for ΔX_{x_i} becomes:

$$\Delta X_{x_i} = \frac{1}{2}\left[d_{x_i} - 2t_{(x_i - \Delta x)}\right] \cdot \Delta S_{x_i} + \left[t_{(x_i + \Delta x)} - t_{(x_i - \Delta x)}\right] \cdot \sum_i \Delta S_{x_i - 1} \tag{3-25}$$

Solving the above for ΔS_{x_i} and substituting in equation (3-19) for

ΔV_{x_i}:

$$\Delta V_{x_i} = \frac{1}{2} d_{x_i} \left[\frac{\Delta X_{x_i} - \left[t_{(x_i + \Delta x)} - t_{(x_i - \Delta x)} \right] \sum_i \Delta S_{x_{i-1}}}{\frac{1}{2} \left[d_{x_i} - 2t_{(x_i - \Delta x)} \right]} \right] \quad (3\text{-}26)$$

which upon simplification becomes:

$$\Delta V_{x_i} = \frac{d_{x_i} \cdot \Delta X_{x_i}}{d_{x_i} - 2t_{(x_i - \Delta x)}} - \frac{d_{x_i} \; t_{(x_i + \Delta x)} - t_{(x_i - \Delta x)} \cdot \sum_i \Delta S_{x_{i-1}}}{d_{x_i} - 2t_{(x_i - \Delta x)}} \quad (3\text{-}27)$$

Now letting

$$R_{x_i} = \frac{d_{x_i}}{d_{x_i} - 2t_{(x_i - \Delta x)}} \quad (3\text{-}28)$$

and

$$R'_{x_i} = R_{x_i} \cdot \left[t_{(x_i + \Delta x)} - t_{(x_i - \Delta x)} \right] \quad (3\text{-}29)$$

the simplified equation for ΔV_{x_i} is obtained in the form:

$$\Delta V_{x_i} = \left[R_{x_i} \cdot \Delta X_{x_i} \right] - \left[R'_{x_i} \cdot \sum_i \Delta S_{x_{i-1}} \right] \quad (3\text{-}30)$$

When all the contributions ΔV_{x_i} and ΔS_{x_i} are summed up, the cumulative volume $\Sigma \Delta V_{x_i}$ and the cumulative surface area $\Sigma \Delta S_{x_i}$ are re-

spectively obtained. The quantity $\Sigma \Delta V_{x_i}$ represents the total volume while $\Sigma \Delta X_{x_i}$ represents the total surface area of the pores which have a width greater than d_x.

It is now necessary to consider the methods of calculation of the basic parameters r_p, d, r_k, and t.

For pores which are assumed to be cylindrical in shape, the value of r_p, the radius of the largest pore filled with liquid nitrogen at any pressure (Figure 2), is given by:

$$r_p = r_k + t \tag{3-4}$$

with r_k and t being, as before, the Kelvin radius and the thickness of the multilayer, respectively.

In the case of "slit-shaped" pores, for which the parallel-plate model has been assumed, the value of d, the maximum distance of wall separation at which capillary condensation can occur at any given relative pressure P/P_o, is represented by the following equation:

$$d = r_k + 2t \tag{3-18}$$

with Figure 3 showing the cross section of the parallel-plate model.

The r_k's are evaluated from the Kelvin equation:

$$\ln \frac{P}{P_o} = - \frac{2\sigma V_m}{RTr_k} \tag{3-1}$$

where the assumption has been made that the contact angle Ψ is 0^o, and so cos Ψ equals unity. This equation can be simplified further when

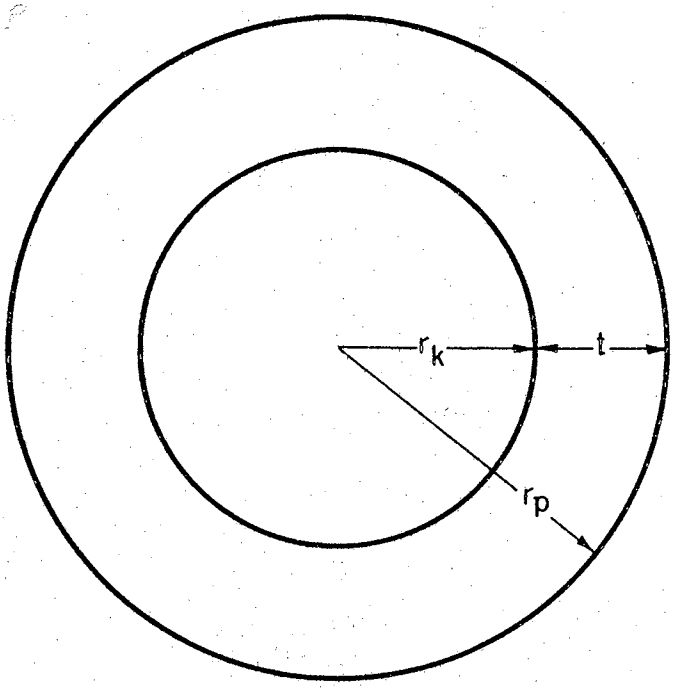

Figure 2. Cross Section of Cylindrical Model

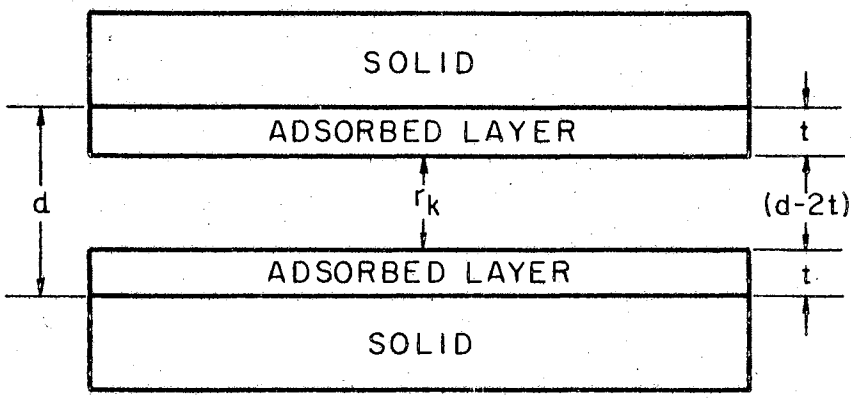

Figure 3. Cross Section of Parallel-Plate Model

nitrogen gas is the adsorbate and adsorption isotherms are obtained at the liquid nitrogen temperature. In this case the values of σ (8.72 dynes/cm), V_m (34.68 cm^3/mole of the liquid), T (78°K), and R (8.316 x 10^7 ergs/°K) when substituted into the Kelvin equation give:

$$\log \frac{P}{P_o} = -\frac{4.14}{r_k} \quad \text{and} \quad r_k = -\frac{4.14}{\log(P/P_o)} \tag{3-31}$$

The layer thickness, t, can be evaluated by either of two methods, one proposed by Shull[10], and the other by De Boer and co-workers[15,16,17].

Shull has taken the BET thicknesses and plotted the experimental values of the number of adsorbed layers versus the relative pressure. The number of adsorbed layers is given as the ratio $(V_{ads.}/V_m)$, where $V_{ads.}$ is the volume adsorbed at any pressure and V_m is the volume corresponding to monomolecular coverage of the surface. In this manner an average adsorption isotherm is obtained. It is obvious that this method does not take into account capillary condensation. Using now the average isotherm the thickness of the adsorbed layer can be calculated as a function of the relative pressure if the assumption is made that the thickness of the monolayer must be equal to the diameter of the nitrogen molecule, taken as 4.3 Å. De Boer points out that Shull's calculation of the t curve is inconsistent because of the fact that when computing the diameter of the nitrogen molecule Shull assumed a closest packing of spheres, while on the other hand, he assumed that the successive layers in multilayer adsorption are packed in such a way that each nitrogen molecule of the following layer is placed just on top of a same molecule of the previous layer.

Lippens, Linsen, and De Boer make the use of a statistical thick-

ness necessary by assuming that both the adsorbed layer and the condensed liquid have the same density, taken as that of the liquid nitrogen. They have defined t as:

$$t = \frac{X}{S} \cdot 10^4 \text{ Å} \tag{3-32}$$

or

$$t = \frac{M \cdot V_{sp}}{22414} \cdot \frac{V_{ads.}}{S} \cdot 10^4 \text{ Å} \tag{3-33}$$

where t is the statistical thickness of the adsorbed layer, X is the adsorbed volume in cm^3 of the liquid adsorbate, S is the specific surface area in m^2/gm of the adsorbent, M is the molecular weight of the adsorbate (28.013 gm/mole of nitrogen), V_{sp} is the specific volume of liquid nitrogen (1.000/0.808 cm^3 per gram), and $V_{ads.}$ is the adsorbed volume of nitrogen gas in cm^3 at S.T.P. per gram of adsorbent. The factor 10^4 is a consequence of the conversion into Angstroms.

When the values for nitrogen are substituted into equation (3-33) the result is:

$$t = 15.47 \cdot \frac{V_{ads.}}{S} \text{ Å} \tag{3-34}$$

The value of S is taken from the BET method which also gives the value V_m, the volume necessary to cover the surface with a unimolecular layer. If the surface area covered by one nitrogen molecule is known then S_{BET} can be calculated from V_m. This surface area is evaluated by assuming a close-packed structure for the adsorbate; in the case of liquid nitrogen it is equal to 16.27 $Å^2$. S_{BET} is then equal to:

$$S_{BET} = 4.37 \cdot V_m \ (m^2/gm) \tag{3-35}$$

and when substituted into equation (3-34) for t gives:

$$t = 3.54 \cdot \frac{V_{ads.}}{V_m} \ \text{Å} \tag{3-36}$$

Thus, either equation (3-34) or equation (3-36) may be used to evaluate the multilayer adsorption thickness t from the data of the BET method at various increments of the relative pressure.

CHAPTER IV

EXPERIMENTAL RESULTS

Three different forms of stannic oxide (SnO_2) are used in this study. The methods of preparation of these materials are given by Rutledge, Kohnke, and Cunningham[18]. Their nitrogen adsorption isotherms were obtained by using a modified BET adsorption apparatus[18].

The stannic oxide powder is a finely divided white substance the particles of which have an average diameter of about 1.5 microns. Powders such as this are expected to be mainly nonporous and in general exhibit an S-shaped isotherm (Brunauer's Type II isotherm). The experimental data for the powder, giving the volume of the nitrogen gas adsorbed with increasing relative pressure, are reproduced in Table I. The corresponding BET nitrogen adsorption-desorption isotherms are represented in Figure 4. The BET equation in its modified form when applied to the isotherm of the powder yields a specific surface area of 1.99 m^2/g[18].

The stannic oxide in the form of a ceramic was prepared from an acetone slurry of the powder[19]. Specific surface areas of ceramics are known to lie below those of their corresponding powders because, as mentioned earlier, the pores present in the powders become smaller in the ceramics during the sintering process. This is shown to be the case for the SnO_2 ceramic. The shape of its isotherm, determined by its pore structure, should follow the general S-shaped isotherm of the powder

and indeed it does. Table I gives the experimental BET adsorption data while Figure 5 represents the adsorption-desorption isotherms of the SnO_2 ceramic. The value of its specific (BET) surface area was found to be equal to 0.37 m^2/g[18].

The third form of stannic oxide under study is the gel. Several methods for the preparation of the gel of various degrees of purity are available[20,21,22,23,24]. A method similar to that reported by Goodman and Gregg[25] was used; it is based upon the hydrolysis of stannic ethoxide. The gel obtained is considered to be ion-free. The experimental data and the adsorption-desorption isotherms are given in Table I and Figure 6, respectively. A Brunauer Type I isotherm is obtained, suggesting that this is a highly porous substance. Application of the BET equation yielded a value of 169 m^2/g for the specific surface area of the gel as compared to the values of 173 m^2/g and 172 m^2/g reported by Rutledge, Kohnke, and Cunningham[18] and by Goodman and Gregg[25], respectively.

In the present investigation the data from the BET nitrogen adsorption isotherms and the BET surface areas are used to compute the pore-size distributions of the three forms of stannic oxide. It should be pointed out that the adsorption data for the powder and the ceramic were taken from Rutledge, Kohnke, and Cunningham[18], which represents previous work done by these investigators on the surface areas of stannic oxide. The adsorption data for the gel were obtained from a more recent experimental run and they are used in this study since they are in excellent agreement with the corresponding data mentioned above. Also to be noted is the fact that the isotherms for all three substances exhibit no hysteresis and they do show the characteristic Type I (Gel) and Type (II)

TABLE I

EXPERIMENTAL DATA

POWDER		CERAMIC		GEL	
P/P_o	$V_{ads.}$	P/P_o	$V_{ads.}$	P/P_o	$V_{ads.}$
0.0124	0.325	0.0195	0.034	0.0124	31.41
0.0210	0.344	0.0361	0.049	0.0181	33.37
0.0332	0.378	0.0671	0.060	0.0252	35.11
0.0466	0.404	0.1136	0.072	0.0321	36.34
0.0593	0.422	0.1733	0.087	0.0373	37.21
0.0677	0.432	0.2264	0.098	0.0402	37.71
0.0844	0.452	0.2607	0.102	0.0885	43.62
0.1466	0.532	0.2956	0.115	0.1121	46.41
0.2416	0.658	0.3264	0.118	0.1290	47.93
0.3471	0.790	0.3903	0.127	0.1393	48.91
0.4425	0.917	0.4735	0.140	0.1446	49.35
0.5040	1.001	0.5140	0.142	0.1544	50.17
0.5662	1.093	0.5797	0.167	0.1696	51.48
0.6339	1.180	0.6684	0.177	0.1887	53.20
0.7110	1.324	0.7831	0.206	0.2372	56.86
0.7979	1.529	0.9096	0.246	0.3358	63.75
0.8176	1.594	0.9885	0.391	0.4350	68.45
0.8499	1.682	0.9101	0.245	0.5184	70.27
0.8902	1.855	0.7830	0.197	0.5195	70.30
0.9235	2.053	0.6695	0.166	0.5561	70.66
0.9595	2.494	0.5801	0.152	0.6980	71.14
0.9860	3.034	0.5151	0.134	0.7857	71.20
0.9560	2.569	0.4710	0.133	0.8757	71.27
0.9207	2.118	0.2792	0.101	0.9969	76.05
0.8882	1.923	0.2395	0.092	0.8760	71.21
0.7974	1.573			0.7863	71.09
0.7684	1.495			0.6975	71.12
0.7144	1.359			0.5547	70.93
0.6144	1.191			0.5173	70.82
0.4168	0.979			0.4011	68.58
0.3951	0.886			0.3663	65.76
0.3464	0.821			0.2126	55.30
0.2724	0.719			0.2030	54.70
0.1892	0.612			0.1812	52.90
0.1149	0.518			0.1470	49.91
0.0952	0.496			0.1073	46.08
0.0460	0.426			0.0694	41.87
0.0288	0.388			0.0425	38.22

$V_{ads.}$ is expressed in cm^3 at S.T.P. per 1 g of adsorbent.

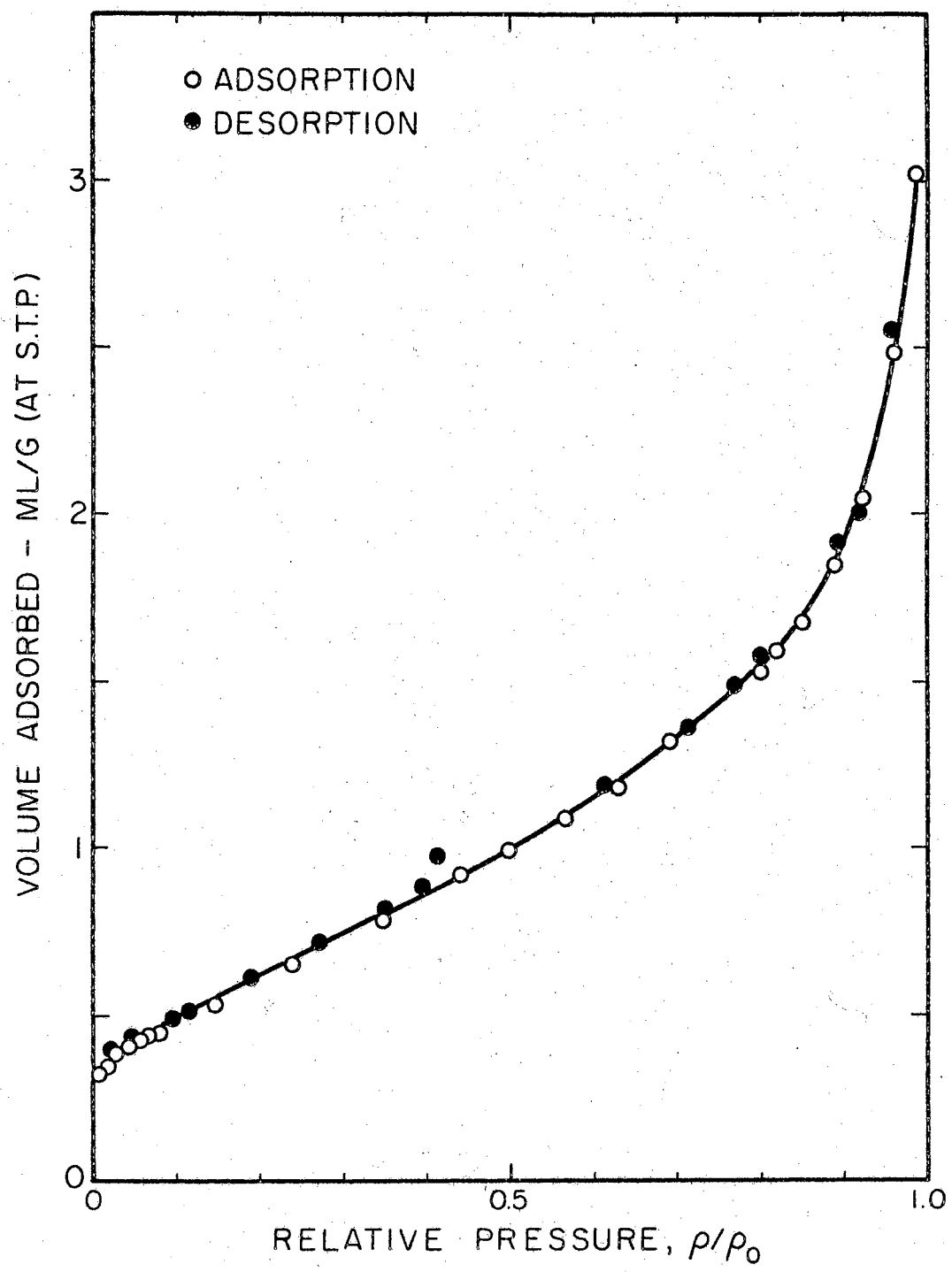

Figure 4. Nitrogen Adsorption Isotherm of SnO_2 Powder at 78°K

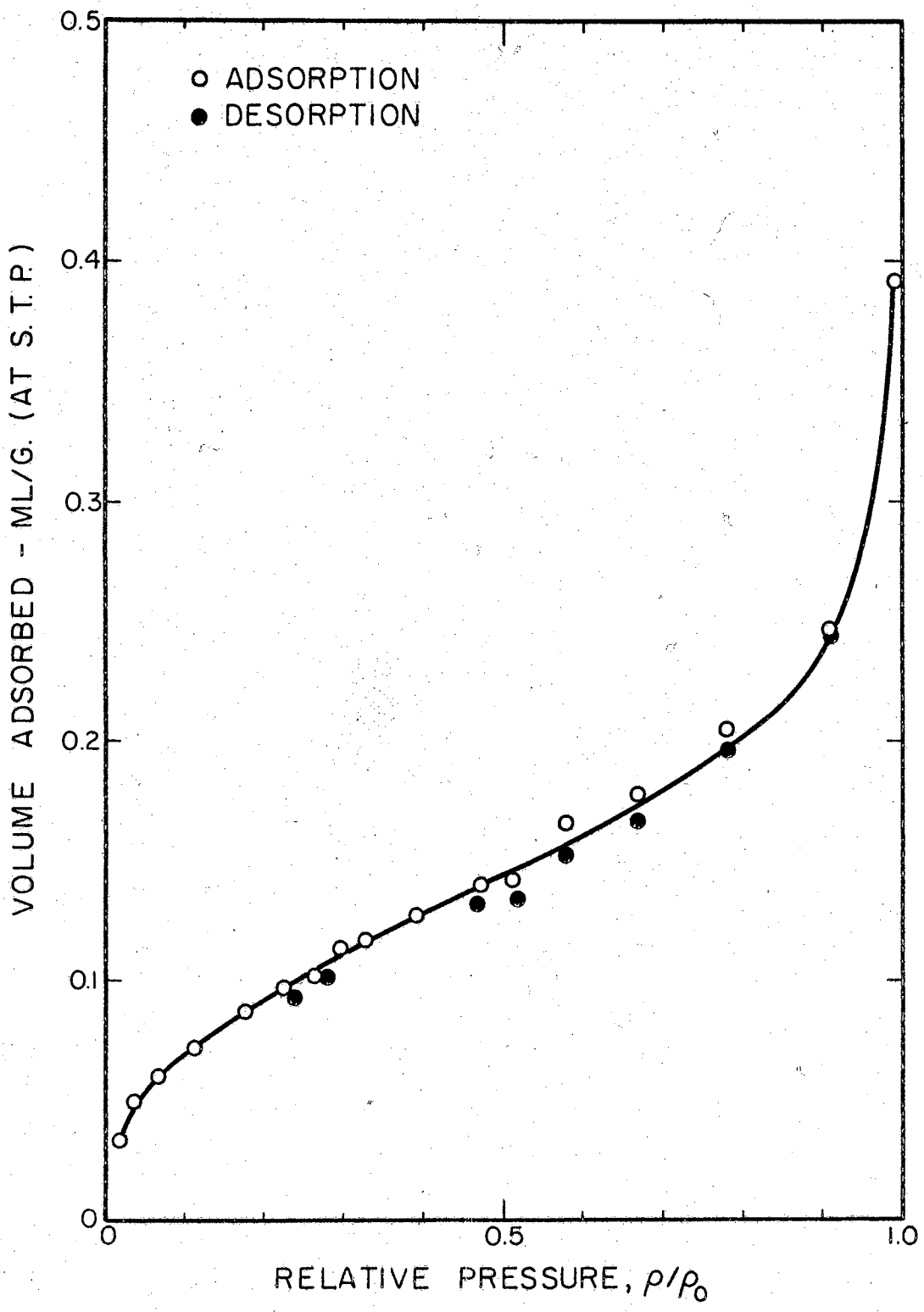

Figure 5. Nitrogen Adsorption Isotherm of SnO_2 Ceramic at 78°K

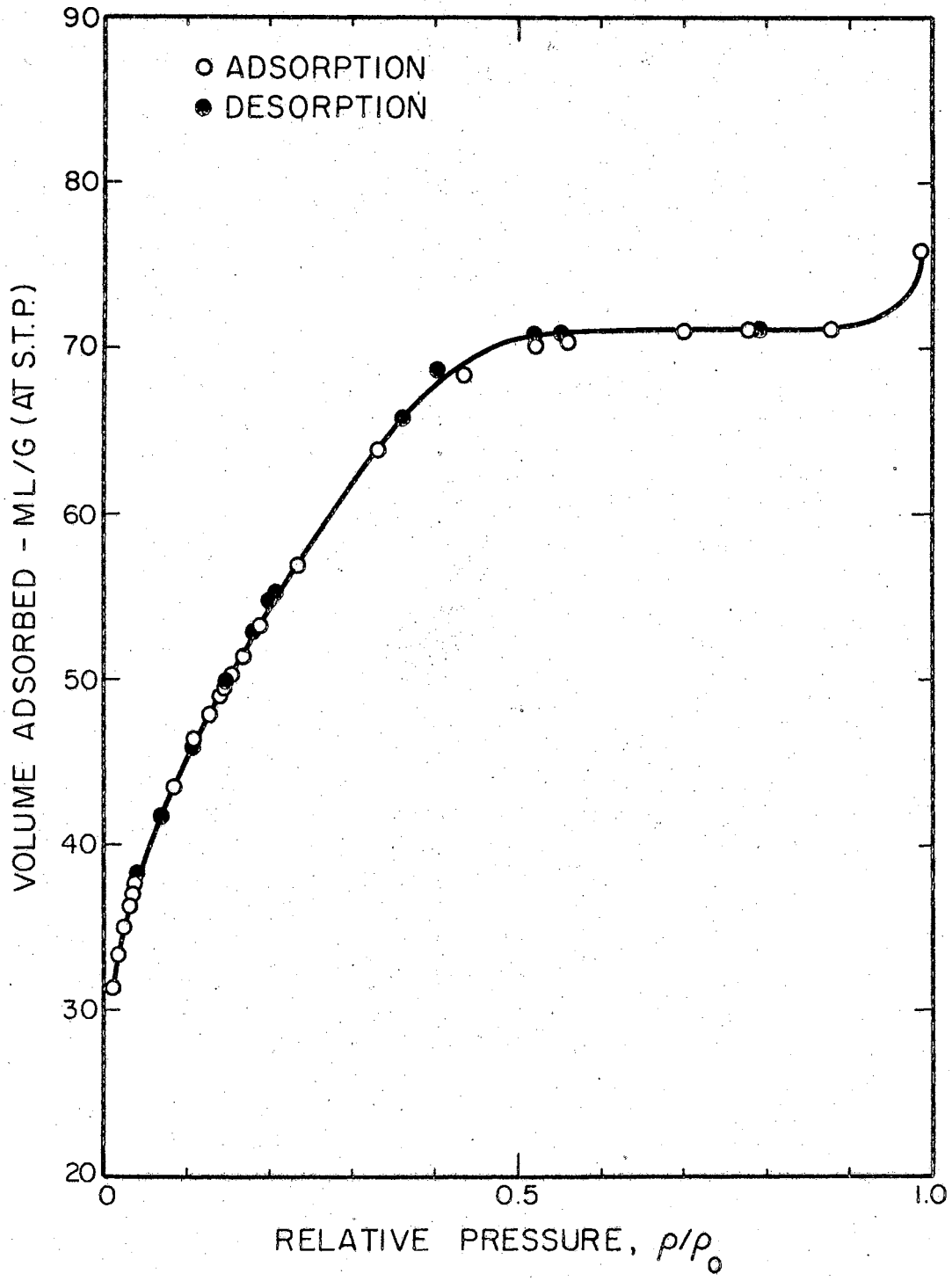

Figure 6. Nitrogen Adsorption Isotherm of SnO_2 Gel at 78°K

(Powder and ceramic) isotherms of Brunauer.

The pores in these materials are assumed to be "slit-shaped" instead of circular, so that the method of calculation as presented by Lippens, Linsen, and De Boer[15] for the parallel-plate model is used and their pore-size distributions are obtained.

The adsorption-desorption isotherms were plotted on an extended scale and then divided into equal increments of the relative pressure. The volume of the gas adsorbed corresponding to each of the pressure increments was read from the graph and used to calculate the values of t from equation (3-34).

The values of the Kelvin radius r_k were calculated from equation (3-31) where P/P_o values are taken as the relative pressure increments.

To evaluate d at each P/P_o the equation $d = r_k + 2t$ was employed. The liquid volumes were computed by multiplying the values of $V_{ads.}$ by 0.00155, which is the factor for converting the volume of gas in cm^3 at S.T.P. to the volume of liquid in cm^3 at its normal boiling point.

The volume of liquid nitrogen desorbed between two consecutive pressure increments is given by ΔX_{x_i}; it is obtained by progressive subtraction of each liquid volume from the succeeding one. ΔX_{x_i} represents the uncorrected distribution for physical adsorption and it is used to calculate the correction factors.

The two correction factors to be evaluated are R_{x_i} and R'_{x_i}, given by equations (3-28) and (3-29), respectively.

Computation of the corrected liquid volume ΔV_{x_i}, the cumulative pore volume $\Sigma \Delta V_{x_i}$, the area of the groups of pores of mean width d_{x_i} ΔS_{x_i}, and the cumulative pore area $\Sigma \Delta S_{x_i}$, must be made from the bottom

to the top, from the largest to the smallest group of pores. The cumulative area $\Sigma\Delta S_{x_{i-1}}$ of all the pores of mean width larger than $d_{(x_i+\Delta x)}$ is used to calculate the correction to the volume of the next lower group of pores of mean width $d_{x_{i-1}}$, etc.

Evaluation of ΔV_{x_i} is made from equation (3-30). For the very last (first from the bottom) group of pores which is also the largest in size this equation becomes:

$$\Delta V_{x_i} = R_{x_i} \cdot \Delta X_{x_i} \tag{4-1}$$

and ΔS_{x_i} is given by:

$$\Delta S_{x_i} = \frac{2\Delta V_{x_i}}{d_{x_i}} \cdot 10^4 \tag{4-2}$$

The presence of the factor 10^{-4} in ΔV_{x_i} and 10^4 in ΔS_{x_i} is accounted for in Appendix A.

The cumulative pore volume $\Sigma\Delta V_{x_i}$ and the cumulative surface area $\Sigma\Delta S_{x_i}$ are obtained by the progressive summing of ΔV_{x_i} and ΔS_{x_i}, respectively, from the bottom to the top.

With the SnO_2 gel as an example a sample calculation will be carried out in order to show the method more clearly and present the mathematical computations involved. These calculations correspond to four groups of pores, two from the bottom and two from the top, with the results given in Table IV.

The values of P/P_o and $V_{ads.}$ are taken from the isotherm of Figure

6 for the gel with the increment of the relative pressure Δx being equal to 0.005. The upper limit for $x = P/P_o$ is 0.655, the value of the pressure at which the isotherm levels off.

The starting point is at $x_1 = 0.010$ with $x_1 - \Delta x = 0.005$ and $x_1 + \Delta x = 0.015$. At $x_1 - \Delta x = 0.005$, $V_{ads.} = 26.40$ cm^3 of nitrogen gas, and $S_{BET} = 169$ m^2/g.

Therefore:

$$t_{(0.005)} = 15.47 \left[\frac{V_{ads.}}{S_{BET}}\right] = 15.47 \left[\frac{26.40}{169}\right] = 2.42 \text{ Å}$$

$$r_{k(0.005)} = -\frac{4.14}{\log x} = -\frac{4.14}{\log(0.005)} = 1.80 \text{ Å}$$

$$d_{(0.005)} = r_{k(0.005)} + 2t_{(0.005)} = 1.80 + 2(2.42) = 6.64 \text{ Å}$$

$$V_{liq.(0.005)} = V_{ads.(o,005)} \cdot (0,00155) =$$

$$= 26.40 \cdot (0.00155) = 0.04092 \text{ cm}^3$$

The same method of calculation is applied to all incremental values of P/P_o up to 0.655. After all four parameters have been evaluated ΔX_{x_i}'s at x_1, x_2, etc., are obtained by successive subtraction. At $x_1 = 0.010$

$$\Delta X_{(0.010)} = V_{liq.(0.015)} - V_{liq.(0.005)}$$

$$= 0.05045 - 0.04092 = 0.00953 \text{ cm}^3$$

Also at $x_1 = 0.010$

$$R_{(0.010)} = \frac{d_{(0.010)}}{d_{(0.010)} - 2t_{(0.005)}} = \frac{7.63}{7.63 - 2(2.42)} = 2.735$$

and

$$R'_{(0.010)} = R_{(0.010)} \cdot \left[t_{(0.015)} - t_{(0.005)} \right] =$$

$$= 2.735 \cdot (2.42 - 2.97) = 1.504$$

The evaluation of ΔX_{x_i}, R_{x_i}, and R'_{x_i} is completed at the relative pressure of x_i equal to 0.650.

In order now to obtain the results given by the last four columns of Table IV, calculations must start from the bottom. Since the pressure at x = 0.650 gives the group of pores in the range of x = 0.645 to x = 0.655, $\Sigma\Delta S$ above x = 0.655 is assumed to be zero. This assumption is not entirely valid because there are some pores of size larger than $d_{(0.655)} = 35.55$ Å which contribute, though slightly, to the over-all surface area. Therefore the correction to the volume $\Delta V_{(0.650)}$ due to $\Sigma\Delta S_{(0.660)}$ represented by the second term of equation (3-30), drops out. The corrected volume is:

$$\Delta V_{(0.650)} = R_{(0.650)} \cdot \Delta X_{(0.650)} =$$

$$= 1.589 \cdot 0.0003 = 0.00005 \text{ cm}^3$$

and $$\Sigma\Delta V_{(0.650)} = 0.00005 \text{ cm}^3$$

Now $$\Delta S_{(0.650)} = \frac{2\Delta V_{(0.650)} \cdot 10^4}{d_{(0.650)}} =$$

$$= \frac{2 \times 4.8 \times 10^{-5} \times 10^4}{35.16} = 0.0270 \text{ m}^2/\text{g}$$

and $$\Sigma\Delta S_{(0.650)} = 0.0270 \ m^2/g$$

This process is repeated for every x_i up to the smaller values at the top of the Table. Contributions to the correction of the volume from the cumulative pore area become more important as x_i decreases. The computations are continued until $\Sigma\Delta V_{x_i}$ reaches the measured volume of the pores which is given at the bottom of the colume for $V_{liq.}$. For the gel this total liquid volume is 0.11028 cm^3 at the relative pressure of 0.655. It is possible to anticipate the step at which the volume will be exhausted. Such a step will give the group containing the smallest pores. In order now to obtain the liquid volume for this group the preceding value of $\Sigma\Delta V$ is subtracted from the measured value of the total volume.

In the cases considered here for the SnO_2 powder, ceramic, and gel it is evident that the volume of the pores is not exhausted even at the very smallest pore sizes. It is necessary at this point to assume that the remaining volume should be adsorbed in pores of sizes larger than the size of the nitrogen molecule but smaller than the size of the smallest pore contained in the group immediately above. If the diameter of the nitrogen molecule is taken as 4.3 Å then this smallest group of pores should have a mean separation d between 4.3 Å and $d_{(x_i - \Delta x)}$.

In the case of the gel (Table IV) at $x_1 = 0.010$:

$$\Delta V_{(0.010)} = \left[R_{(0.010)} \cdot \Delta x_{(0.010)} \right] - \left[R'_{(0.010)} \cdot \Sigma\Delta S_{(0.020)} \cdot 10^{-4} \right] = \tag{4-3}$$

$$= (2.735 \times 0.00953) - (1.504 \times 130.43 \times 10^{-4}) =$$

$$= 0.00644 \text{ cm}^3$$

$$\Sigma\Delta V_{(0.010)} = \Sigma\Delta V_{(0.020)} + \Delta V_{(0.010)} =$$

$$= 0.09856 + 0.00644 = 0.10500 \text{ cm}^3$$

$$\Delta S_{(0.010)} = \frac{2 \times \Delta V_{(0.010)} \times 10^4}{d_{(0.010)}} =$$

$$= \frac{2 \times 0.00644 \times 10^4}{7.63} = 16.90 \text{ m}^2/\text{g}$$

$$\Sigma\Delta S_{(0.010)} = \Sigma \Delta S_{(0.020)} + \Delta S_{(0.010)} =$$

$$= 130.43 + 16.90 = 147.33 \text{ m}^2/\text{g}$$

It is observed that the group of pores at $x_1 = 0.010$ has not exhausted the total liquid volume. The over-all volume desorbed when the relative pressure is reduced to 0.005 is 0.10500 cm^3. The volume which remains is given by:

$$\Delta V_{(x < 0.005)} = V_{liq.(0.655)} - \Sigma\Delta V_{(0.010)} =$$

$$= 0.11028 - 0.10500 = 0.00528 \text{ cm}^3$$

and it is the volume of the pores having d between 4.3 Å and 6.64 Å. An average separation equal to 5.47 Å is used to evaluate $\Delta S_{(x < 0.005)}$ for the group of pores at P/P_o equal to or less than 0.005.

Thus

$$\Delta S_{(x < 0.005)} = \frac{2 \times \Delta V_{(x < 0.005)} \times 10^4}{d_{(x < 0.005)}} =$$

$$= \frac{2 \times 0.00528 \times 10^4}{5.47} = 19.31 \text{ m}^2/\text{g}$$

and the cumulative surface area $\Sigma\Delta S$ will then be:

$$\Sigma\Delta S = \Sigma\Delta S_{(0.010)} + \Delta S_{(x < 0.005)} =$$

$$= 147.33 + 19.31 = 166.64 \text{ m}^2/\text{g}$$

Therefore the total surface area of the gel obtained by the method of pore-size distribution has the value of 167 m^2/g.

The same sequence of calculations is employed for the powder and the ceramic forms of stannic oxide. Evaluation of the pore-size distribution in the powder was carried out at a relative pressure reaching an upper limit of 0.987, while for the ceramic an upper limit of 0.990 is used. This is necessary because of the shape of their isotherms.

Tables II, III, and IV give part of the results of the pore-size distribution calculations for the SnO_2 powder, ceramic and gel, respectively. Table V presents selected values of the cumulative pore volume $\Sigma\Delta V$ and the cumulative surface area $\Sigma\Delta S$ with the corresponding values of the pore-wall separation d for all three substances. Plots of the cumulative pore volume versus d_{x_i} are represented in Figures 7, 8, and 9, while plots of the cumulative surface area versus d_{x_i} are given in Figures 10, 11, and 12.

After all computations have been completed, all the ΔV_{x_i}'s can be divided by the Δd's over which they were determined. The resulting values of $\Delta V/\Delta d$ are then plotted against the corresponding d_{x_i}'s in order to obtain the differential pore-volume distribution curves

TABLE II

COMPUTATION OF PORE VOLUME AND AREA DISTRIBUTIONS FOR STANNIC OXIDE POWDER

P/P_o	$V_{ads.}$	t	r_k	d	$V_{liq.}$	ΔX_{x_i}	R_{x_i}	R'_{x_i}	ΔV_{x_i}	$\Sigma\Delta V_{x_i}$	ΔS_{x_i}	$\Sigma\Delta S_{x_i}$
-----	-----	----	----	5.65	--------	--------	-----	-----	0.000033	0.004715	0.1170	1.9700
0.010	0.315	2.45	2.07	6.97	0.000488	--------	-----	-----	--------	--------	------	------
0.020	0.362	2.81	2.44	8.06	--------	0.000120	2.551	1.530	0.000036	0.004682	0.0890	1.8530
0.030	0.392	3.05	2.72	8.82	0.000608	--------	-----	-----	--------	--------	------	------
0.040	0.413	3.21	2.96	9.38	--------	0.000063	2.860	0.915	0.000023	0.004646	0.0490	1.7640
0.050	0.433	3.37	3.18	9.92	0.000671	--------	-----	-----	--------	--------	------	------
0.060	0.449	3.49	3.39	10.37	--------	0.000048	2.857	0.687	0.000022	0.004623	0.0423	1.7150
0.070	0.464	3.61	3.58	10.80	0.000719	--------	-----	-----	--------	--------	------	------
0.080	0.477	3.71	3.77	11.19	--------	0.000039	2.819	0.536	0.000023	0.004601	0.0411	1.6727
0.090	0.489	3.80	3.96	11.56	0.000758	--------	-----	-----	--------	--------	------	------
0.100	0.501	3.89	4.14	11.92	--------	0.000036	2.759	0.497	0.000020	0.004578	0.0336	1.6316
0.110	0.512	3.98	4.32	12.28	0.000794	--------	-----	-----	--------	--------	------	------
0.120	0.523	4.07	4.50	12.64	--------	0.000037	2.701	0.513	0.000020	0.004558	0.0316	1.5980
0.130	0.536	4.17	4.67	13.01	0.000831	--------	-----	-----	--------	0.004538	------	1.5664
.	.	.	.	.	.	.	.	.	.	.	.	.
.	.	.	.	.	.	.	.	.	.	.	.	.
0.945	2.332	18.13	168.30	204.60	0.003615	--------	-----	-----	--------	--------	------	------
0.950	2.396	18.63	185.70	223.00	--------	0.000269	1.194	1.612	0.000313	0.001245	0.0281	0.0801
0.955	2.506	19.48	207.00	246.00	0.003884	--------	-----	-----	--------	--------	------	------
0.960	2.622	20.38	233.90	275.00	--------	0.000301	1.165	1.759	0.000346	0.000932	0.0252	0.0520
0.965	2.700	20.99	267.00	309.00	0.004185	--------	-----	-----	--------	--------	------	------
0.970	2.782	21.63	314.00	357.00	--------	0.000240	1.133	1.360	0.000270	0.000586	0.0151	0.0268
0.975	2.855	22.19	377.00	421.00	0.004425	--------	-----	-----	--------	--------	------	------
0.977	2.880	22.39	410.00	455.00	--------	0.000101	1.108	0.565	0.000112	0.000316	0.0049	0.0117
0.979	2.920	22.70	450.00	495.00	0.004526	--------	-----	-----	--------	--------	------	------
0.981	2.950	22.93	499.00	545.00	--------	0.000093	1.091	0.458	0.000101	0.000204	0.0037	0.0068
0.983	2.980	23.12	560.00	606.00	0.004619	--------	-----	-----	--------	--------	------	------
0.985	3.010	23.40	627.00	674.00	--------	0.000096	1.074	0.569	0.000103	0.000103	0.0031	0.0031
0.987	3.042	23.65	726.00	774.00	0.004715	--------	-----	------	--------	--------	------	------

TABLE III

COMPUTATION OF PORE VOLUME AND AREA DISTRIBUTIONS FOR STANNIC OXIDE CERAMIC

P/P_o	$V_{ads.}$	t	r_k	d	$V_{liq.}$	ΔX_{x_i}	R_{x_i}	R'_{x_i}	ΔV_{x_i}	$\Sigma\Delta V_{x_i}$	ΔS_{x_i}	$\Sigma\Delta S_{x_i}$
-----	-----	----	----	4.80	--------	--------	-----	-----	0.000004	0.000605	0.0170	0.3480
0.020	0.034	1.42	2.44	5.28	0.000053	--------	-----	-----	--------	--------	------	------
0.030	0.044	1.84	2.72	6.40	--------	0.000025	1.798	1.204	0.000008	0.000601	0.0255	0.3310
0.040	0.050	2.09	2.96	7.14	0.000078	--------	-----	-----	--------	--------	------	------
0.050	0.054	2.26	3.18	7.70	--------	0.000012	2.188	0.744	0.000005	0.000593	0.0130	0.3055
0.060	0.058	2.43	3.39	8.25	0.000090	--------	-----	-----	--------	--------	------	------
0.070	0.061	2.55	3.58	8.68	--------	0.000010	2.272	0.568	0.000007	0.000588	0.0160	0.2925
0.080	0.064	2.68	3.77	9.13	0.000100	--------	-----	-----	--------	--------	------	------
0.090	0.067	2.80	3.96	9.56	--------	0.000009	2.276	0.569	0.000005	0.000581	0.0113	0.2765
0.100	0.070	2.93	4.14	10.00	0.000009	--------	-----	-----	--------	--------	------	------
0.110	0.073	3.05	4.32	10.42	--------	0.000007	2.285	0.480	0.000004	0.000576	0.0077	0.2652
0.120	0.075	3.14	4.50	10.78	0.000116	--------	-----	-----	--------	--------	------	------
0.130	0.077	3.22	4.67	11.11	--------	0.000006	2.300	0.368	0.000005	0.000572	0.0085	0.2575
0.140	0.079	3.30	4.85	11.45	0.000122	--------	-----	-----	--------	0.000567	------	0.2490
.	.	.	.	.	.	.	.	.	.	.	.	.
.	.	.	.	.	.	.	.	.	.	.	.	.
0.960	0.308	12.86	234.00	260.00	0.000477	--------	-----	-----	--------	--------	------	------
0.965	0.316	13.22	267.00	294.00	--------	0.000031	1.096	0.931	0.000034	0.000136	0.0023	0.0062
0.970	0.328	13.71	314.00	341.00	0.000508	--------	-----	-----	--------	--------	------	------
0.972	0.332	13.88	334.00	364.00	--------	0.000014	1.081	0.411	0.000015	0.000102	0.0008	0.0039
0.974	0.337	14.09	363.00	391.00	0.000522	--------	-----	-----	--------	--------	------	------
0.976	0.342	14.31	391.00	419.00	--------	0.000016	1.072	0.472	0.000017	0.000087	0.0008	0.0031
0.978	0.347	14.53	427.00	456.00	0.000538	--------	-----	-----	--------	--------	------	------
0.980	0.354	14.80	471.00	500.00	--------	0.000020	1.062	0.552	0.000021	0.000070	0.0009	0.0023
0.982	0.360	15.05	524.00	554.00	0.000558	--------	-----	-----	--------	--------	------	------
0.984	0.367	15.34	591.00	622.00	--------	0.000025	1.051	0.704	0.000026	0.000049	0.0008	0.0014
0.986	0.376	15.72	679.00	710.00	0.000583	--------	-----	-----	--------	--------	------	------
0.988	0.386	16.14	796.00	828.00	--------	0.000022	1.039	0.613	0.000023	0.000023	0.0006	0.0006
0.990	0.390	16.50	941.00	974.00	0.000605	--------	-----	-----	--------	--------	------	------

TABLE IV

COMPUTATION OF PORE VOLUME AND AREA DISTRIBUTIONS FOR STANNIC OXIDE GEL

P/P_o	$V_{ads.}$	t	r_k	d_{x_i}	$V_{liq.}$	ΔX_{x_i}	R_{x_i}	R'_{x_i}	ΔV_{x_i}	$\Sigma\Delta V_{x_i}$	ΔS_{x_i}	$\Sigma\Delta S_{x_i}$
-----	-----	-----	----	5.47	-------	-------	-----	------	0.00528	0.11028	19.310	166.640
0.005	26.40	2.420	1.80	6.64	0.04092	-------	-----	------	-------	-------	------	-------
0.010	30.30	2.780	2.07	7.63	-------	0.00953	2.735	1.5041	0.00644	0.10500	16.900	147.330
0.015	32.55	2.970	2.27	8.21	0.05045	-------	-----	------	-------	-------	------	-------
0.020	34.00	3.090	2.44	8.62	-------	0.00410	3.216	0.7398	0.00427	0.09856	9.904	130.430
0.025	35.20	3.200	2.58	8.98	0.05455	-------	-----	------	-------	-------	------	-------
0.030	36.10	3.300	2.72	9.32	-------	0.00287	3.192	0.5745	0.00255	0.09429	5.475	120.526
0.035	37.05	3.380	2.84	9.60	0.05742	-------	-----	------	-------	-------	------	-------
0.040	37.90	3.450	2.96	9.86	-------	0.00249	3.181	0.4771	0.00269	0.09174	5.460	115.051
0.045	38.65	3.530	3.07	10.13	0.05991	-------	-----	------	-------	-------	------	-------
0.050	39.43	3.600	3.18	10.38	-------	0.00217	3.127	0.4064	0.00253	0.08905	4.875	109.591
0.055	40.05	3.660	3.29	10.61	0.06208	-------	-----	------	-------	-------	------	-------
0.060	40.80	3.720	3.39	10.83	-------	0.00209	3.085	0.3703	0.00276	0.08652	5.095	104.716
0.065	41.40	3.780	3.49	11.05	0.06417	-------	-----	------	-------	0.08376	------	99.621
.	.	.	.	.	.	.	.	.	.	.	.	.
.	.	.	.	.	.	.	.	.	.	.	.	.
0.595	71.03	6.502	18.36	31.36	0.11010	-------	-----	------	-------	-------	------	-------
0.600	71.04	6.504	18.67	31.68	-------	0.00003	1.696	0.0034	0.00005	0.00030	0.032	0.177
0.605	71.05	6.506	18.97	31.98	0.11013	-------	-----	------	-------	-------	------	-------
0.610	71.06	6.507	19.28	32.29	-------	0.00003	1.675	0.0033	0.00005	0.00025	0.031	0.145
0.615	71.07	6.508	19.61	32.63	0.11016	-------	-----	------	-------	-------	------	-------
0.620	71.08	6.509	19.94	32.96	-------	0.00003	1.653	0.0033	0.00005	0.00020	0.030	0.114
0.625	71.09	6.510	20.29	33.31	0.11019	-------	-----	------	-------	-------	------	-------
0.630	71.10	6.511	20.63	33.65	-------	0.00003	1.631	0.0033	0.00005	0.00015	0.029	0.084
0.635	71.11	6.512	20.99	34.02	0.11022	-------	-----	------	-------	-------	------	-------
0.640	71.12	6.513	21.36	34.39	-------	0.00003	1.610	0.0032	0.00005	0.00010	0.028	0.055
0.645	71.13	6.514	21.74	34.77	0.11025	-------	-----	------	-------	-------	------	-------
0.650	71.14	6.515	22.13	35.16	-------	0.00003	1.589	0.0032	0.00005	0.00005	0.027	0.027
0.655	71.15	6.516	22.52	35.55	0.11028	-------	-----	------	-------	-------	------	-------

TABLE V

CUMULATIVE PORE VOLUME AND CUMULATIVE SURFACE AREA

POWDER			CERAMIC			GEL		
d	$\Sigma\Delta V$	$\Sigma\Delta S$	d	$\Sigma\Delta V$	$\Sigma\Delta S$	d	$\Sigma\Delta V$	$\Sigma\Delta S$
5.65	0.004715	1.9700	4.80	0.000605	0.3480	5.47	0.11028	166.640
8.06	0.004682	1.8530	7.70	0.000593	0.3055	7.63	0.10500	147.330
10.37	0.004623	1.7150	10.42	0.000576	0.2652	8.62	0.09856	130.430
12.64	0.004558	1.5980	12.58	0.000560	0.2372	9.86	0.09174	115.051
15.60	0.004456	1.4504	14.85	0.000539	0.2052	11.26	0.09376	99.620
18.81	0.004328	1.2980	17.06	0.000518	0.1780	12.08	0.07949	92.162
22.35	0.004163	1.1340	21.00	0.000493	0.1407	13.18	0.07237	80.741
27.44	0.003925	0.9384	24.52	0.000456	0.1164	14.22	0.06522	70.159
32.33	0.003716	0.7950	27.78	0.000433	0.0992	15.24	0.05781	59.967
40.46	0.003432	0.6338	31.73	0.000411	0.0841	16.19	0.05111	51.355
50.34	0.003152	0.5065	36.77	0.000387	0.0693	17.52	0.04274	41.325
57.61	0.002959	0.4324	46.43	0.000350	0.0508	18.78	0.03413	31.757
67.29	0.002744	0.3605	63.03	0.000309	0.0348	20.14	0.02560	22.905
81.32	0.002494	0.2894	87.62	0.000278	0.0259	21.69	0.01769	15.247
103.80	0.002186	0.2177	115.82	0.000250	0.0199	22.54	0.01241	10.440
132.80	0.001838	0.1545	143.84	0.000226	0.0160	23.33	0.00698	5.665
165.30	0.001587	0.1185	164.48	0.000210	0.0138	24.08	0.00326	2.496
189.30	0.001440	0.1007	192.00	0.000189	0.0112	24.81	0.00186	1.341
223.00	0.001245	0.0801	232.00	0.000166	0.0088	25.93	0.00136	0.938
274.70	0.000932	0.0520	294.00	0.000136	0.0062	28.00	0.00086	0.562
356.80	0.000586	0.0268	364.00	0.000102	0.0039	30.49	0.00040	0.245

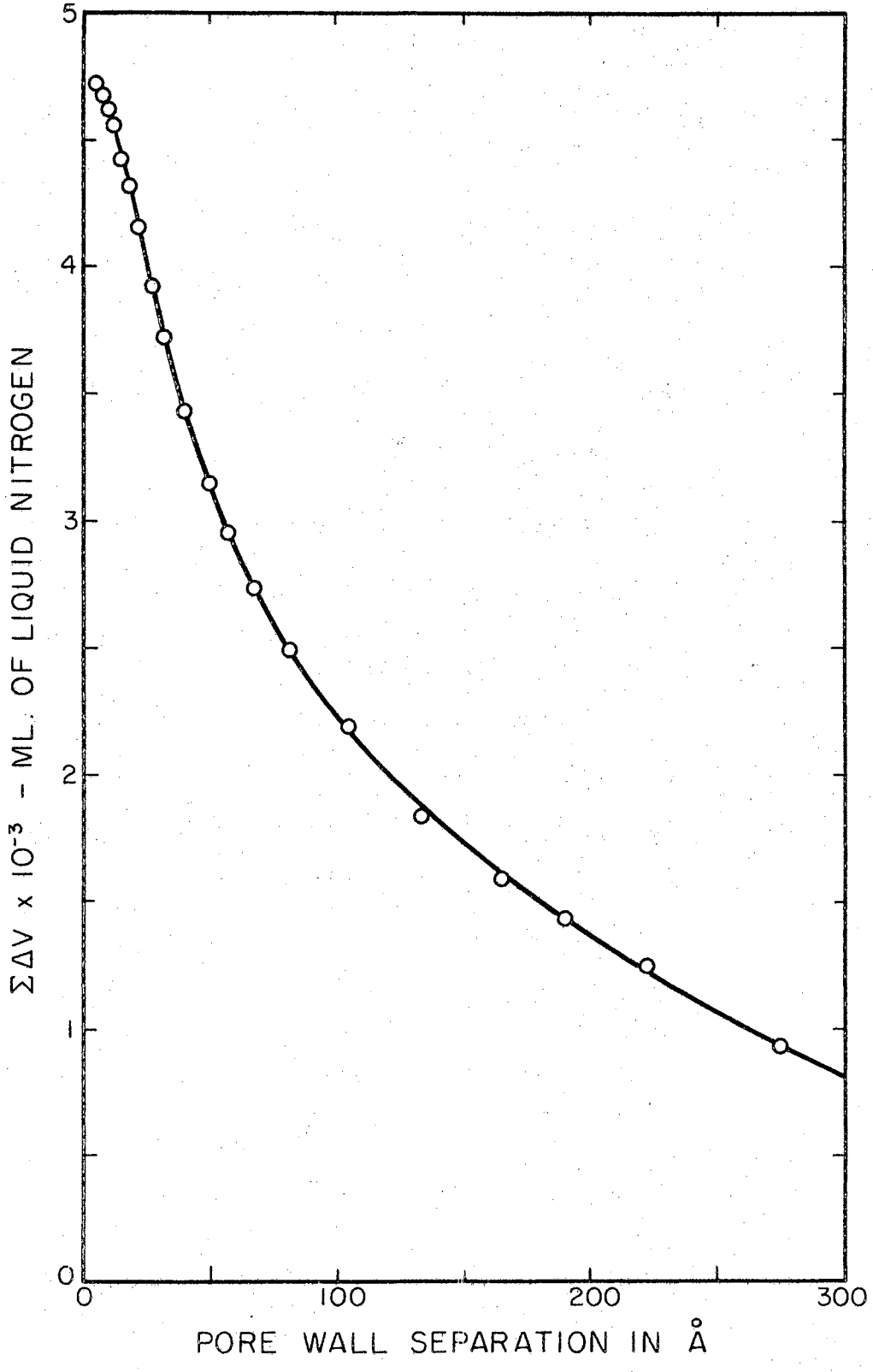

Figure 7. Cumulative Pore-Volume Curve for SnO_2 Powder

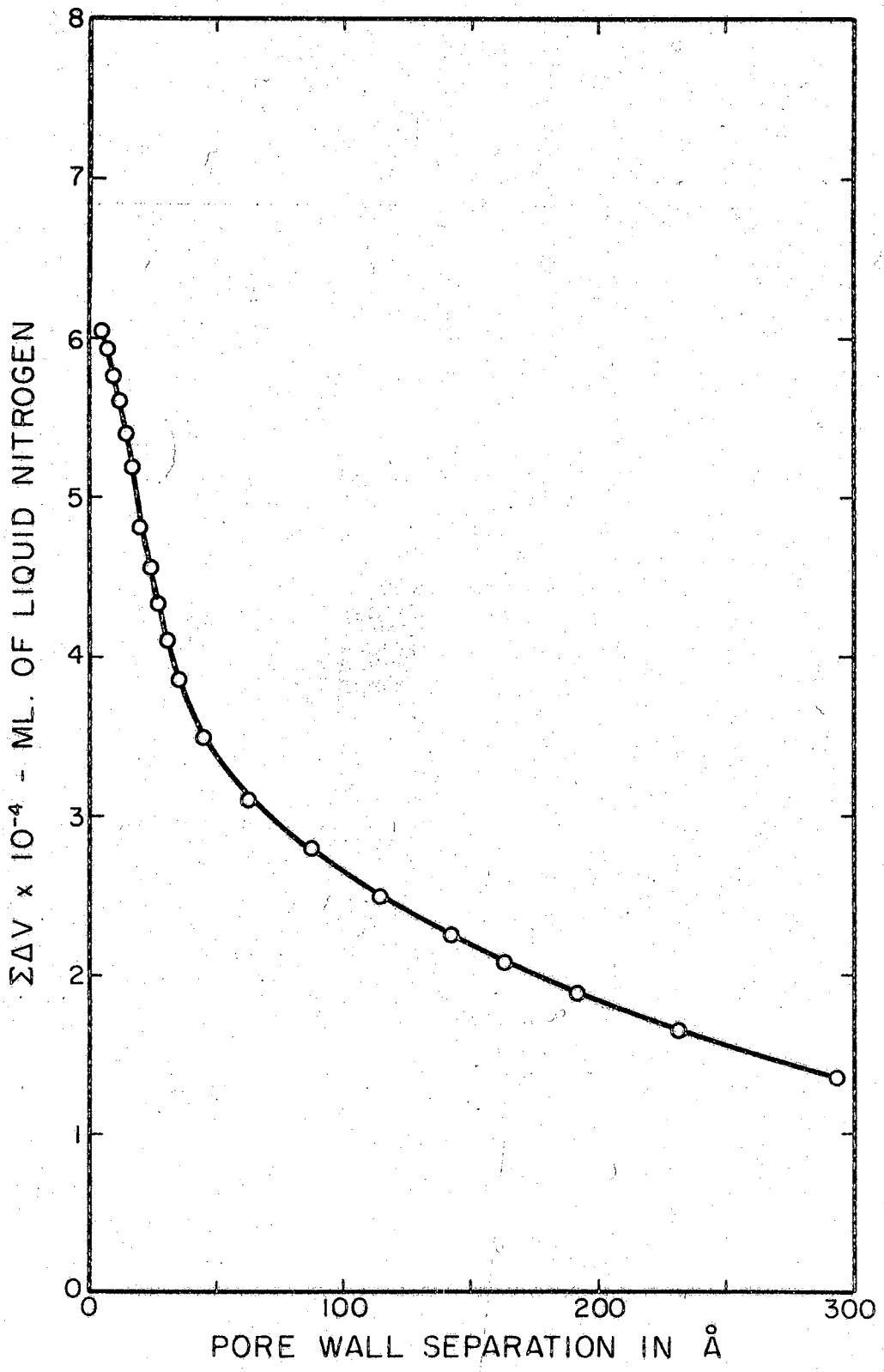

Figure 8. Cumulative Pore-Volume Curve for SnO_2 Ceramic

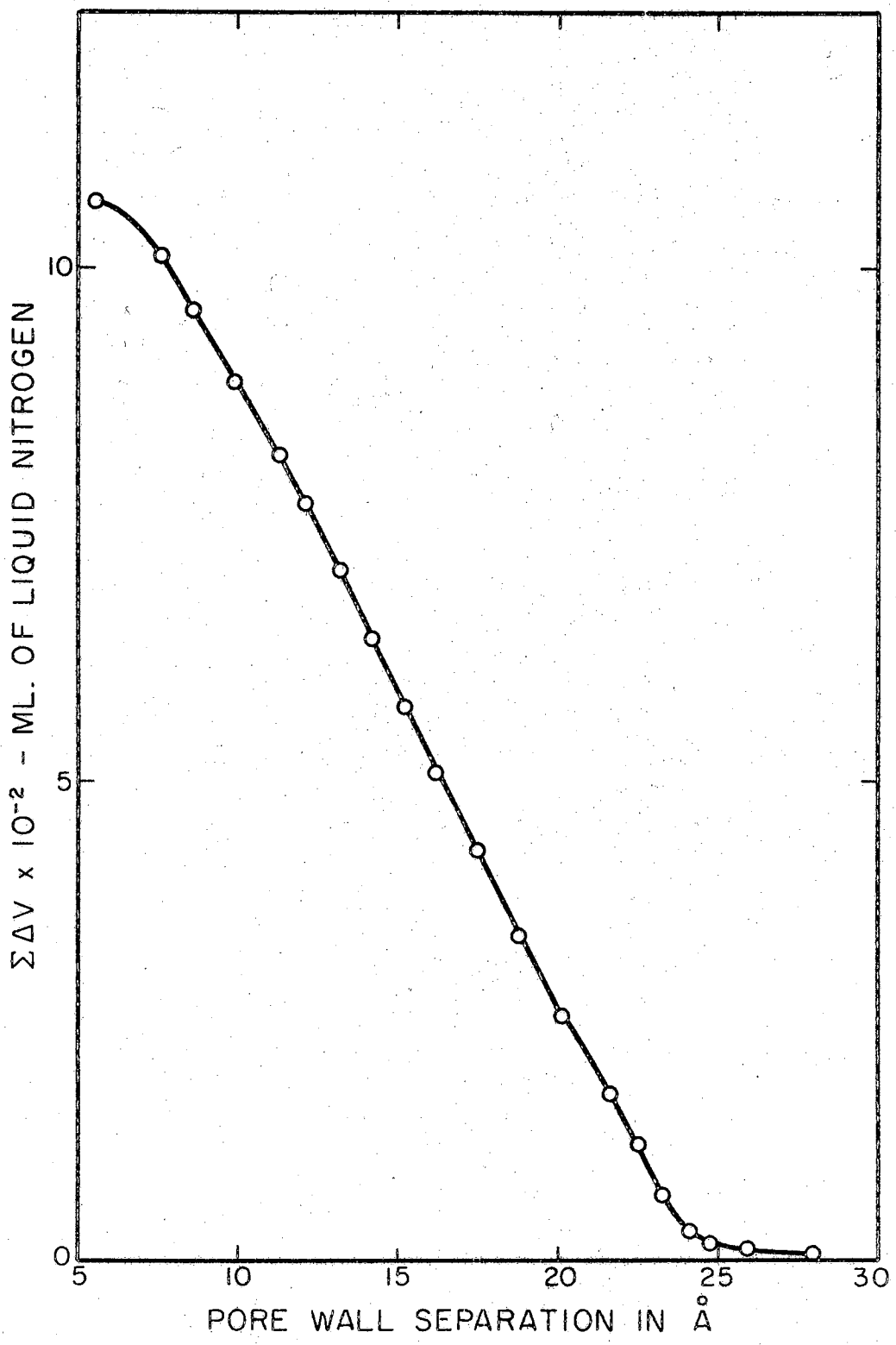

Figure 9. Cumulative Pore-Volume Curve for SnO_2 Gel

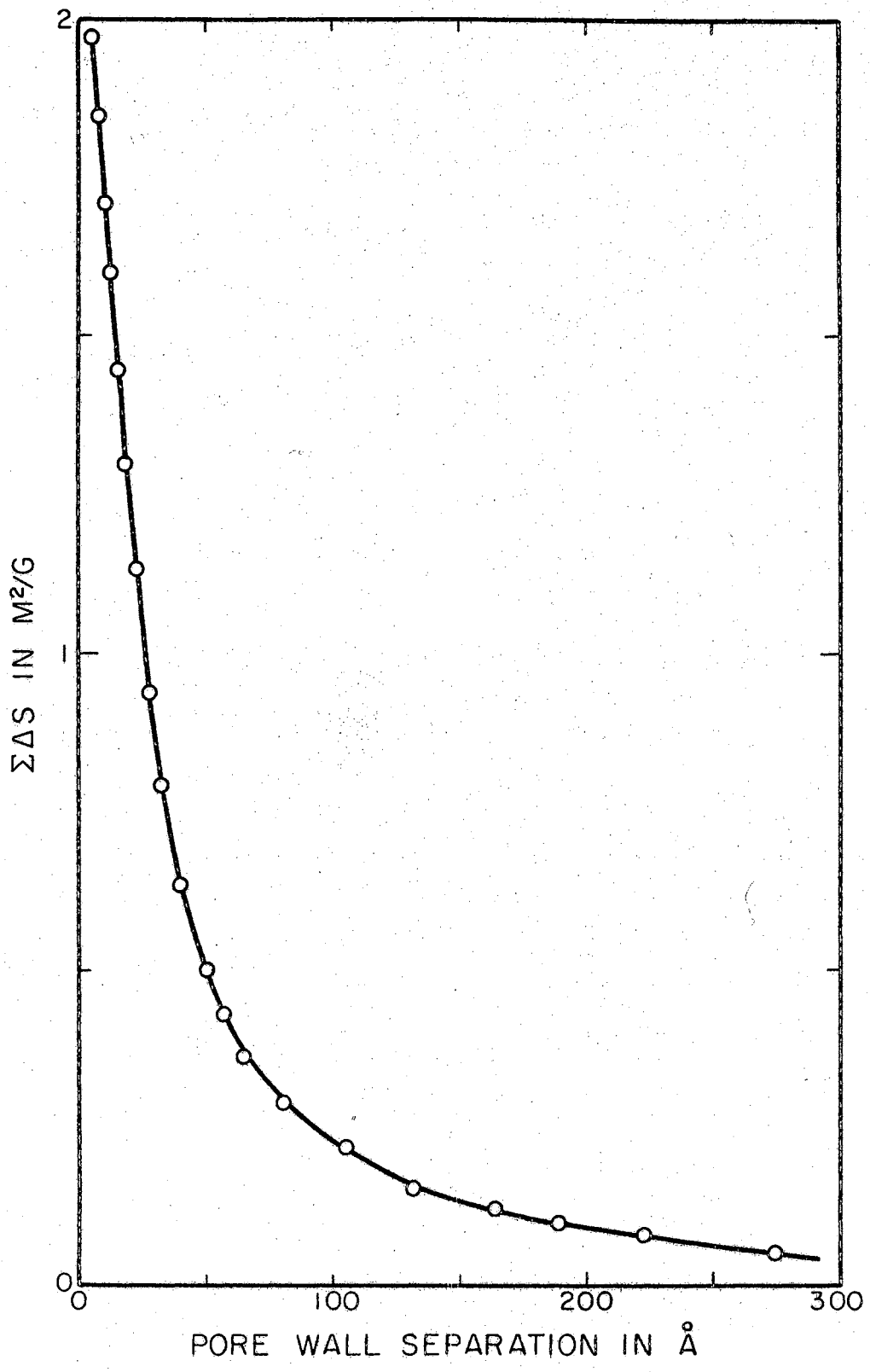

Figure 10. Cumulative Surface Area Curve for SnO_2 Powder

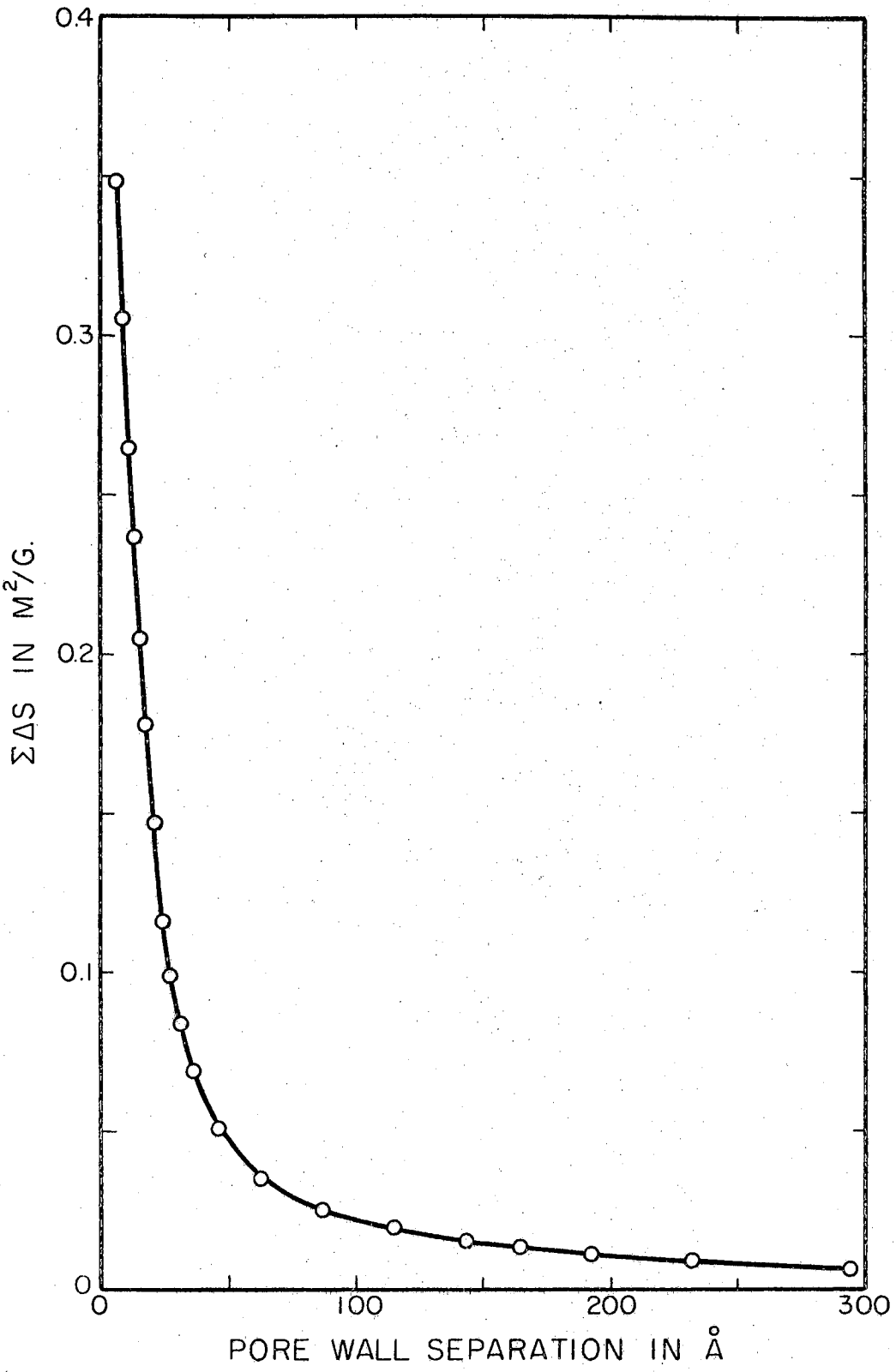

Figure 11. Cumulative Surface Area Curve for SnO_2 Ceramic

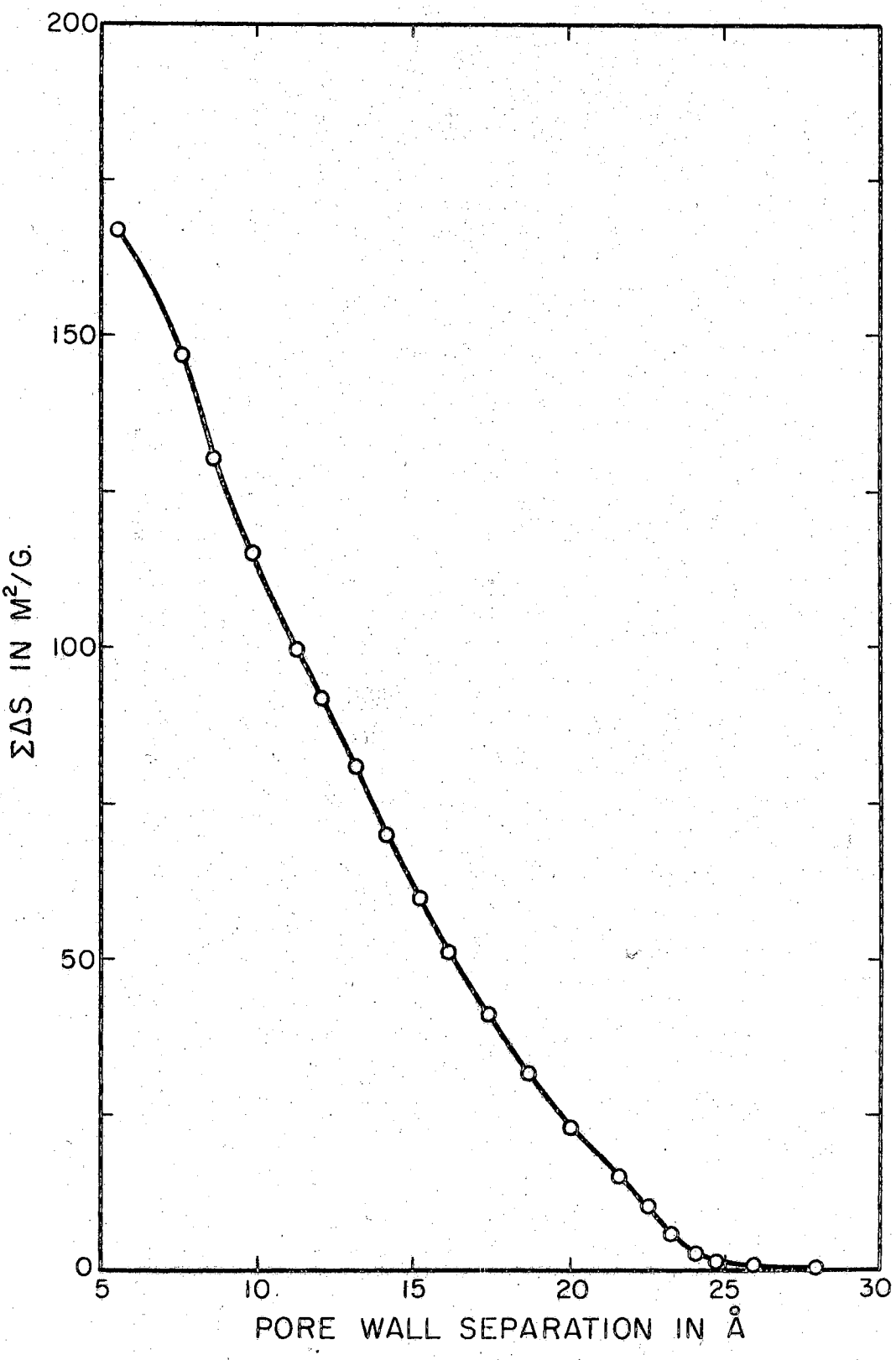

Figure 12. Cumulative Surface Area Curve for SnO_2 Gel

(Appendix B). In Table VI selected values of $\Delta V/\Delta d$ versus d_{x_i} have been recorded to give relatively smooth distribution curves for the three forms of stannic oxide, which are represented in Figures 13, 14, and 15 for the powder, the ceramic, and the gel, respectively. These curves indicate the location of the pore-volume maxima, showing at the same time the range of the pore separation in which most of the adsorption occurs.

When $\Sigma\Delta V_{x_i}$ equals the measured volume of the pores, then $\Sigma\Delta S_{x_i}$ should be in good agreement with the total surface area computed from the BET method. These two values should check well within an experimental error of approximately 5 per cent.

It is worth mentioning at this point that pore-size distributions for SnO_2 gel were computed on the basis of the method of Barrett, Joyner, and Halenda[9] for cylindrical pores. Average pore radii $\bar{r}_p$ were taken between the values of 5.5 Å and 24.5 Å. Several sets of calculations corresponding to various values of the constant c which appears in this method were carried out. Cumulative surface area computed in this manner were unsatisfactory when compared to the BET surface area. The best agreement that could be obtained, for the gel, occurred at values of c equal to 0.5 and 0.6 with the surface area having values of 200 m^2/g and 206 m^2/g, respectively. When compared to the BET results the above areas show an error of between 18 and 20 per cent. Thus the Barrett, Joyner, and Halenda method of circular pore radii was rejected as unsatisfactory because of the magnitude of the per cent error.

TABLE VI

DIFFERENTIAL PORE VOLUME DISTRIBUTION

POWDER		CERAMIC		GEL	
d	$(\Delta V/\Delta d)\times10^{-5}$	d	$(\Delta V/\Delta d)\times10^{-6}$	d	$(\Delta V/\Delta d)\times10^{-3}$
5.65	1.24	4.80	4.00	5.47	2.30
8.06	1.95	7.70	4.50	7.63	4.10
10.37	2.50	8.68	7.95	8.62	5.50
11.19	3.03	11.80	9.09	10.83	6.30
13.39	3.33	13.34	11.63	13.18	7.30
14.86	3.85	16.32	12.00	14.22	7.50
15.60	4.05	20.13	11.63	14.90	7.50
18.00	4.38	23.56	8.25	15.88	7.30
21.44	5.23	26.62	8.11	18.16	7.20
25.29	4.95	28.99	7.09	18.78	7.00
27.44	4.55	36.77	5.21	19.80	6.10
32.33	4.30	41.02	4.22	20.14	5.80
33.74	3.79	46.43	3.57	20.52	5.50
35.24	3.55	49.71	3.15	20.88	5.40
38.54	3.30	57.79	2.10	21.69	5.30
44.82	2.95	63.03	1.75	22.13	6.80
57.61	2.52	69.32	1.40	22.96	7.30
67.29	2.09	77.24	1.22	23.33	6.60
73.52	1.90	87.62	1.08	23.71	3.50
81.32	1.74	101.66	0.91	24.08	2.40
103.80	1.30	128.24	1.13	24.50	1.40
119.20	1.03	143.84	0.90	24.81	0.66
132.80	0.93	164.50	0.90	25.18	0.39
147.20	0.89	192.00	0.70	25.93	0.32
189.30	0.69	232.00	0.60	27.12	0.22
274.70	0.55	294.00	0.42	28.93	0.15
356.80	0.24	364.00	0.30	29.95	0.10
455.00	0.15	500.00	0.21	32.29	0.08
674.00	0.06	828.00	0.09	34.39	0.06

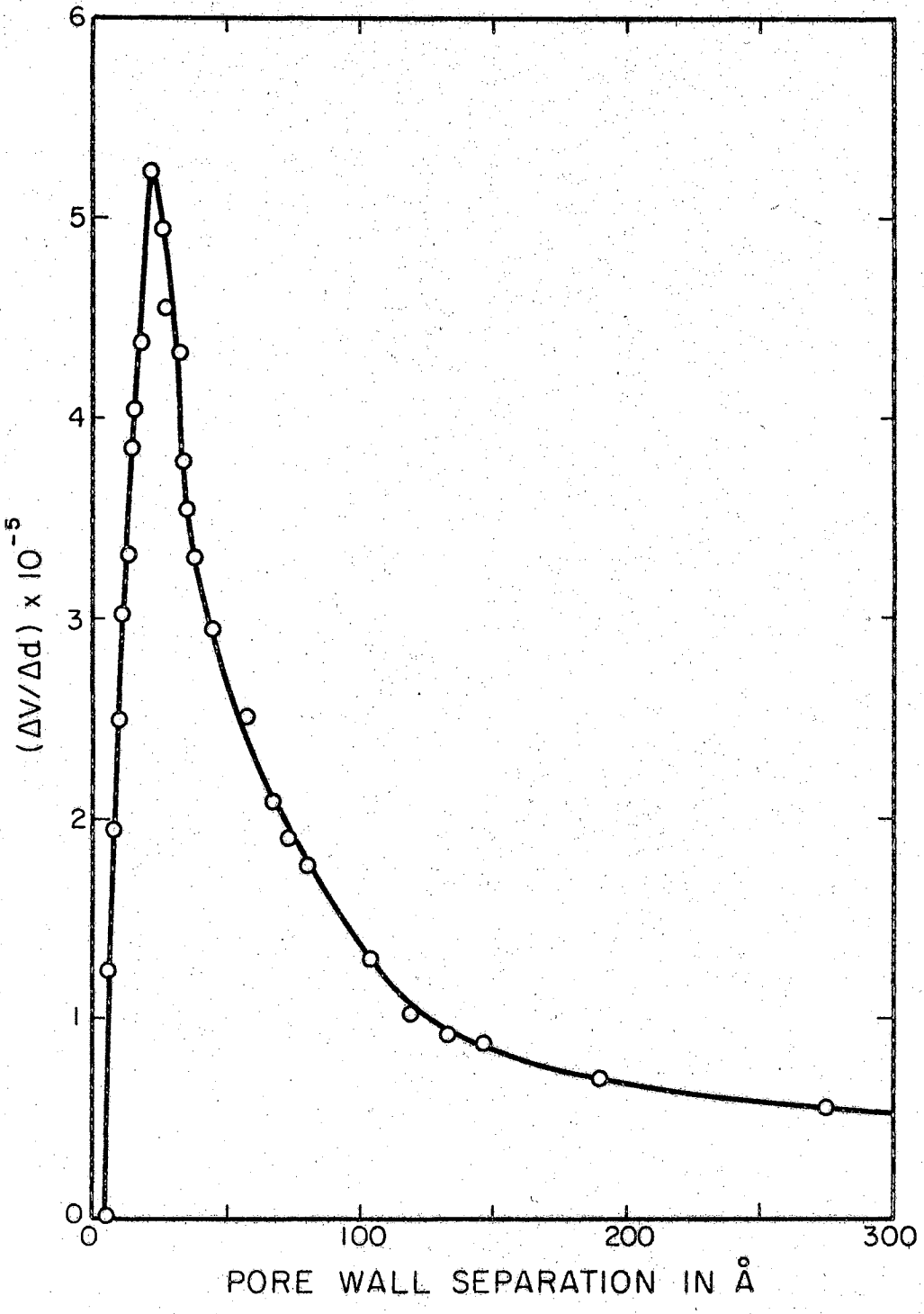

Figure 13. Differential Pore-Volume Distribution Curve for SnO_2 Powder

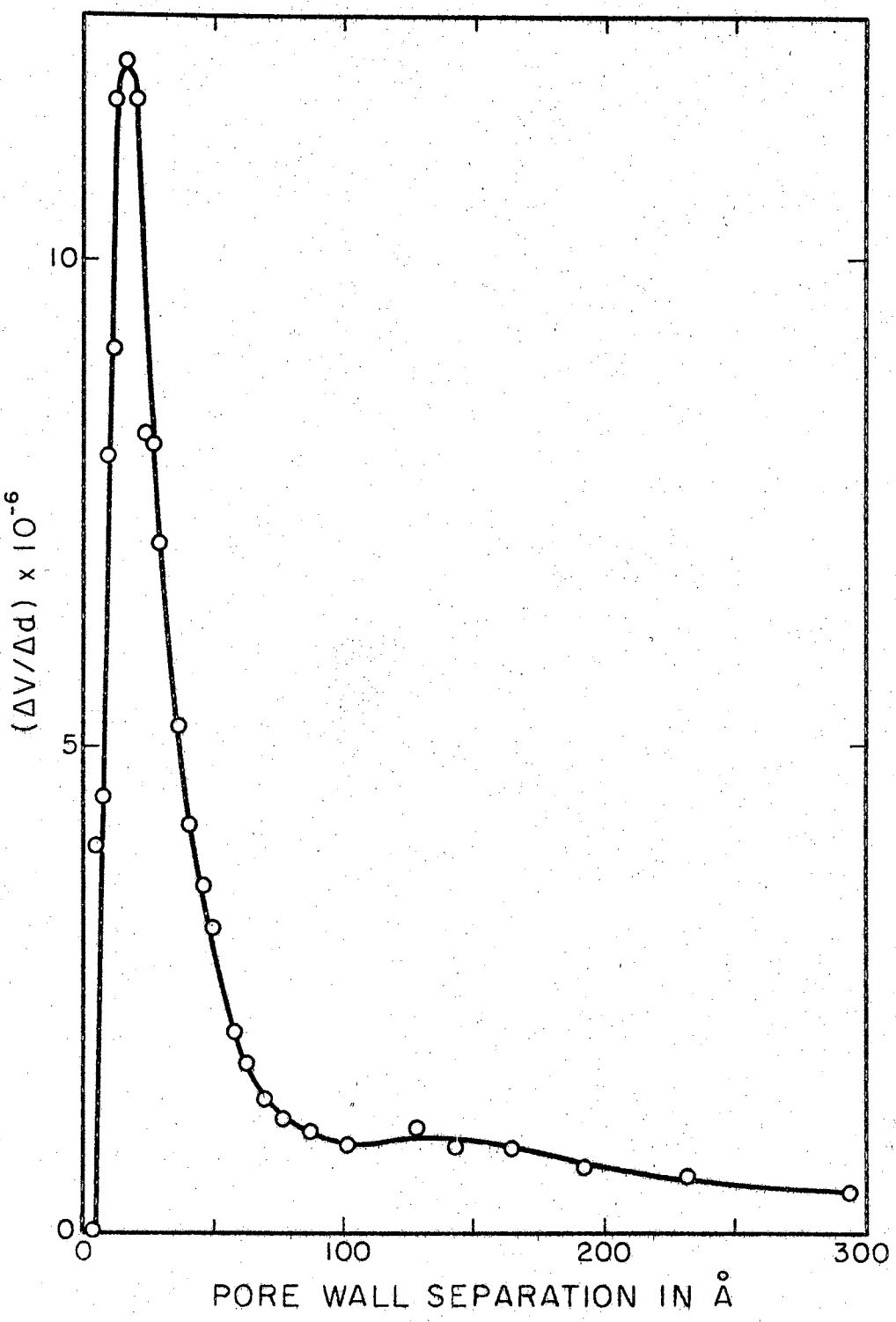

Figure 14. Differential Pore-Volume Distribution Curve for SnO_2 Ceramic

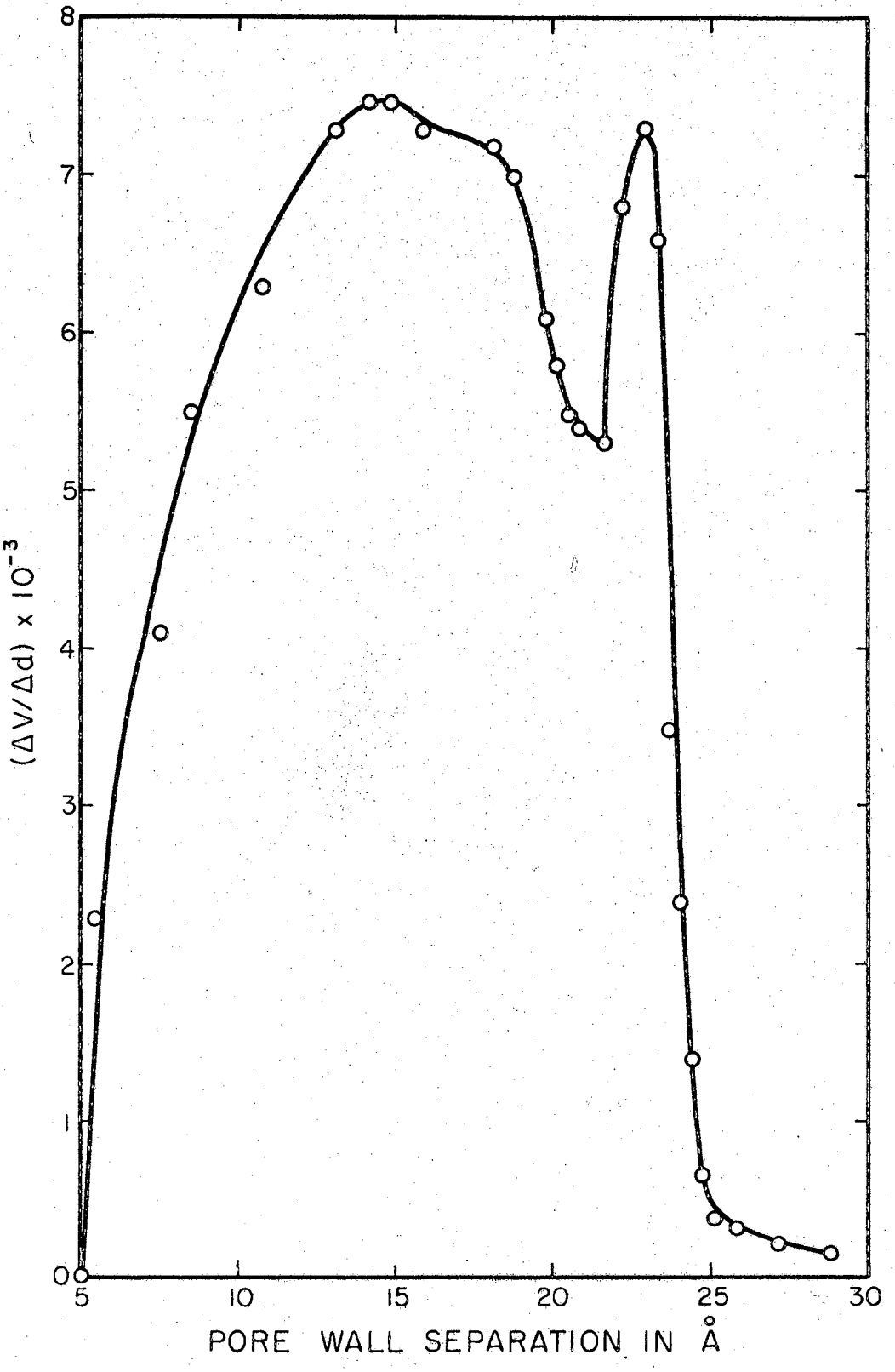

Figure 15. Differential Pore-Volume Distribution Curve for SnO_2 Gel

CHAPTER V

CONCLUSIONS

From theoretical considerations the type of adsorption isotherm depends on the presence or absence of pores in solid adsorbents[7,8]. The adsorption properties of the powder and the ceramic forms of stannic oxide appear to be quite similar since they both exhibit the same type of isotherm. Therefore pore-size distributions should also be of a similar nature for both. It is further expected that the pores in the ceramic should be smaller than those in the powder.

The powder exhibits an S-shaped adsorption isotherm which is characteristic of nonporous solids. As emphasized earlier, this type of isotherm does not preclude the presence of pores in such substances entirely and it is necessary to employ other means in order to obtain information as to the existence and nature of these pores. Such information becomes available from the calculations on pore-size distributions.

From the differential pore-volume distribution curve of the powder, represented in Figure 13, the presence of pores is very much in evidence. Pore-wall separations in the powder start at about 5 Å and range all the way up to separations of 1000 Å and over. Most of the pores present have values of d between 5 Å and 125 Å. The maximum volume of nitrogen is being adsorbed by the group of pores with a wall separation of about 20 Å. Pores having sizes larger than 125 Å contribute considerably to the overall surface area of the powder.

The results obtained for the stannic oxide ceramic are, as expected, very similar to those of the powder. From the differential pore volume distribution of Figure 14 it is observed that pores of size of 5 Å and larger are present in the solid. Most of the pores appear to be in the range of 5 Å to 75 Å with the pore-volume maximum occurring at about 15 Å. These pores are very prominent and their contribution to the total surface area is considerable. It is observed that their size, being smaller than that for the powder, is consistent with the fact that on sintering decrease in the pore-wall separation is expected.

The results for both the powder and the ceramic are in accordance with the considerations derived from the shapes of their adsorption isotherms. The lack of hysteresis on the S-shaped isotherm indicates that no appreciable number of pores should be present at higher relative pressures. At lower pressures, on the other hand, capillary condensation sets in, as shown by the pore-volume maxima of Figures 13 and 14, giving evidence of the presence of pores obtained from the distribution curves. This is in perfect agreement with the assumption that the S-shaped isotherm, although characteristic for nonporous substances, does not exclude the presence of capillaries along with the "flat" or "free" surface of such solids.

The effect of these pores will be shown in terms of their contribution to the total volume adsorbed and to the total surface area of the powder and the ceramic. When the former is considered, approximately 58 per cent of the volume is taken up by pores which have wall separations of 125 Å or less and the remaining is attributed to pores larger than 125 Å. For the latter, about 52 per cent of the volume is adsorbed by pores of 75 Å or less. Surface areas due to these pores

contribute at higher percentages to the total because of their smaller size. About 90 per cent of the area of the powder comes from the pores up to 125 Å, while about 85 per cent of the area of the ceramic is due to pores up to 75 Å.

When the total surface areas obtained from the present method of pore size distribution are compared with those from the BET method, a very close and satisfactory agreement is observed. The area of the powder from this method has the value of 1.97 m^2/gm as compared to the value of 1.99 m^2/gm from the BET[18], with an error of 1 per cent. For the ceramic a surface area of 0.35 m^2/gm from the distribution method when compared to the BET[18] value of 0.37 m^2/gm shows an error of 5.4 per cent, in good agreement with the experimental error.

The BET Type I experimental adsorption isotherm of the stannic oxide gel points out that this is a highly porous substance. The pore-size distribution results are in complete agreement with the theoretical observations from the shape of the isotherm. Figures 9 and 12, which represent the cumulative pore-volume and cumulative surface area curves, respectively, show a definite break at a value of about 25 Å for the average pore wall separation of the gel. The starting point of these curves is located at 5.5 Å. As the value of d increases the curves level off and become asymptotic to the d-axis, indicating that no significant amount of gas is adsorbed by pores larger than 25 Å. The amount of volume in pores of size between 5.5 Å and 25 Å makes up 98.5 per cent of the total adsorbed volume, while the surface area of these pores comprises 99 per cent of the total surface area of the gel. The curve for the differential pore-volume distribution is represented in Figure 15 with the origin at 5.5 Å and the same definite break shown

to occur at 25 Å. Two maxima are observed, the first at 14-15 Å and the second at 23 Å.

If the value of 167 m^2/g for the total surface area of the gel is compared with the BET result of 169 m^2/g a remarkable agreement is observed. The error is only 1.2 per cent.

From the foregoing discussion, it is concluded that the gel is a highly porous substance with about 99 per cent of the pores having sizes between 5.5 Å and 25 Å.

If now the cumulative pore-volume, cumulative surface area, and differential pore-volume distribution curves of the powder and the ceramic are compared with those of the gel, it is evident that no definite breaks occur with increasing values of the pore wall separation. These curves decrease exponentially and reach the d-axis asymptotically as d becomes large. For these two substances, therefore, no definite pore-size distribution exists, but their pores range in values from about 5 Å all the way up to and beyond 1000 Å, with an appreciable number of them being in the range of 5 Å to 125 Å for the powder and 5 Å to 75 Å for the ceramic.

Further work on the stannic oxide gel is possible because it is a very good adsorbent and as such it can be used in IR studies. It is also transparent in the form of thin (1 mm) plates and transmits infrared radiation. Such studies are now being carried out. They will include IR absorption spectra of the gel at room temperature and atmospheric pressure, at room temperature under vacuum, at liquid hydrogen temperature ($20^{\circ}K$) under vacuum, and at liquid hydrogen temperature with certain gases (such as hydrogen gas) adsorbed on the surface. In order to achieve the low temperature of liquid hydrogen a cryostat is

used and it is designed in such a way as to fit the IR-7 infra-red spectrophotometer.

BIBLIOGRAPHY

1. Brunauer, S., Emmett, P. H. and Teller, E., J. Am. Chem. Soc. 60, 309 (1938).

2. Harkins, W. D. and Jura, G., J. Chem. Phys. 11, 431 (1943).

3. Cohan, L. A., J. Am. Chem. Soc. 60, 433 (1938).

4. Brunauer, S., The Adsorption of Gases and Vapors, Vol. I, Physical Adsorption, Princeton Univ. Press, Princeton (1945).

5. Wheeler, A., Presentations at Catalysis Symposia, Gibson Island, AAAS Conferences, June 1945 and June 1946.

6. Wheeler, A., Catalysis, Emmett, P. H., ed., Vol. 2, Reinhold, New York (1955).

7. Carman, P. C., J. Phys. Chem. 57, 56 (1953).

8. Pierce, C. and Smith, R. N., J. Phys. Chem. 57, 64 (1953).

9. Barrett, E. P., Joyner, L. G. and Halenda, P. P., J. Am. Chem. Soc. 73, 373 (1951).

10. Shull, C. G., J. Am. Chem. Soc. 70, 1405 (1948).

11. Oulton, T. D., J. Phys. Colloid Chem. 52, 1296 (1948).

12. Anderson, R. B., J. Catalysis, 3, 50 (1964).

13. Inness, W. B., Anal. Chem. 29, 1069 (1957).

14. De Boer, J. H., Proceedings of the Tenth Symposium of the Colston Research Society held in the University of Bristol, The Structure and Properties of Porous Materials, Butterworths, London (1958).

15. Lippens, B. C., Linsen, B. G. and De Boer, J. H., J. Catalysis, 3, 32 (1964).

16. De Boer, J. H. and Lippens, B. C., J. Catalysis, 3, 38 (1964).

17. Lippens, B. C. and De Boer, J. H., J. Catalysis, 3, 44 (1964).

18. Rutledge, J. L., Kohnke, E. E. and Cunningham, C. M., Interim Report SS-2, NASA Grant NsG609, Research Foundation, Oklahoma

State University, Stillwater, December 1965.

19. Matthews, H. E., Unpublished M.S. Thesis, Oklahoma State University (1965).

20. Dhar, N. R. and Varadanam, Ch. I., J. Indian Chem. Soc. 13, 602 (1936).

21. Aditya, S., J. Indian Chem. Soc. 29, 296 (1952).

22. Ghosh, B. N. and Ghosh, A. K., J. Indian Chem. Soc. 34, 871 (1957).

23. Zsigmondy, Annalen 301, 361 (1898).

24. Weiser, H. B., Millican, W. O. and Simpson, W. C., J. Phys. Chem. 46, 1051 (1942).

25. Goodman, J. F. and Gregg, S. J., J. Chem. Soc. (London), 1162 (1960).

APPENDIX A

JUSTIFICATION OF THE FACTOR (10^4) IN EQUATION FOR ΔS_{x_i}

The factor (10^4) which appears in ΔS_{x_i} is introduced in the equation as a conversion factor. This is necessary because ΔV_{x_i} is given in units of (cm^3/g) while d_{x_i} is given in units of angstroms ($\mathring{A}$) as:

$$\Delta S_{x_i} = \left[\frac{2\Delta V_{x_i}}{d_{x_i}}\right] \cdot \left[\frac{cm^3}{\mathring{A} \cdot gm}\right]$$

The units of ΔS_{x_i} have to be expressed in (m^2/g). Therefore:

$$\Delta S_{x_i} = \left[\frac{2\Delta V_{x_i}}{d_{x_i}}\right] \cdot \left[\frac{cm^2 \cdot cm}{\mathring{A} \cdot g}\right]$$

$$= \left[\frac{2\Delta V_{x_i}}{d_{x_i}}\right] \left[\frac{10^{-4} \cdot m^2 \times 10^8 \cdot \mathring{A}}{\mathring{A} \cdot g}\right]$$

$$\Delta S_{x_i} = \left[\frac{2\Delta V_{x_i}}{d_{x_i}}\right] \cdot \left[\frac{10^4 \cdot m^2}{g}\right]$$

When ΔV_{x_i} is computed the units on $\Sigma \Delta S_{x_{i-1}}$ have to be converted to the original units; therefore $\Sigma \Delta S_{x_{i-1}}$ is now multiplied by a factor of 10^{-4} as it appears in equation (4-3).

APPENDIX B

EVALUATION OF DIFFERENTIAL PORE-VOLUME DISTRIBUTION

A sample calculation will be carried out for the stannic oxide gel in order to exemplify the evaluation of $\Delta V/\Delta d$ shown in Table VI.

From Table IV the following data are obtained:

For the smallest group of pores for which $\frac{P}{P_o} \leq 0.005$

$$d_{aver.} = 5.47 \text{ Å}$$

and

$$d_{lim.} = 4.30 \text{ Å}$$

where $d_{lim.}$ is the limiting nitrogen molecule diameter.

Also

$$d_{(0.005)} = 6.64 \text{ Å}$$

At $d_{aver.}$

$$\Delta V_{(x \leq 0.005)} = 0.00528 \text{ cm}^3$$

It follows that

$$\frac{\Delta V}{\Delta d} = \frac{\Delta V_{(x \leq 0.005)}}{d_{(0.005)} - d_{lim.}}$$

$$\frac{\Delta V}{\Delta d} = \frac{0.00528}{6.64 - 4.30} = 2.26 \times 10^{-3} \text{ cm}^3/\text{Å}$$

For the next group of pores at $\frac{P}{P_o} = 0.010$ and $0.005 \leq \frac{P}{P_o} \leq 0.015$, the following data are obtained:

$$d_{(0.010)} = d_{aver.} = 7.63 \text{ Å}$$

$$d_{(0.005)} = 6.64 \text{ Å}$$

$$d_{(0.015)} = 8.21 \text{ Å}$$

$$\Delta V_{(0.010)} = 0.00644 \text{ cm}^3$$

Thus

$$\frac{\Delta V}{\Delta d} = \frac{\Delta V_{(0.010)}}{d_{(0.015)} - d_{(0.005)}}$$

$$\frac{\Delta V}{\Delta d} = \frac{0.00644}{8.21 - 6.64} = 4.10 \times 10^{-3} \text{ cm}^3/\text{Å}$$

This type of calculation is continued up to and including the last (largest) group of pores. It is carried out in the same manner for the powder and the ceramic.

VITA

Theodoros Galaction Vernardakis

Candidate for the Degree of

Master of Science

Thesis: PORE-SIZE DISTRIBUTION OF STANNIC OXIDE IN POWDER, CERAMIC AND GEL FORMS

Major Field: Chemistry

Biographical:

Personal Data: Born in Limassol, Cyprus, November 14, 1942, the son of Galaction G. and Heleni G. Vernardakis.

Education: Graduated from Lanition, Limassol Greek Gymnasium in Limassol, Cyprus, in 1961; received a Bachelor of Science degree from the College of Emporia, Emporia, Kansas, with majors in Chemistry and Mathematics, in May, 1965.